Research Square

Preprints are preliminary reports that have not undergone peer review.
They should not be considered conclusive, used to inform clinical practice,
or referenced by the media as validated information.

BMI modifies the prognostic value of blood urea nitrogen in elderly patients with HFpEF:a retrospective cohort study

Yanyan Li

liyykz@163.com

Air Force Medical University

Hengyi Xue

Air Force Medical University

Xingman Fan

Air Force Medical University

Haitao Zhang

Air Force Medical University

Yanjie Cao

Air Force Medical University

Research Article

Keywords: heart failure with preserved ejection fraction, nutritional assessment, body mass index, geriatric nutritional risk index, blood urea nitrogen, risk stratification

Posted Date: September 24th, 2026

DOI: https://doi.org/10.21203/rs.3.rs-10642977/v1

License: This work is licensed under a Creative Commons Attribution 4.0 International License.
Read Full License

Additional Declarations: No competing interests reported.

TITLES

BMI modifies the prognostic value of blood urea nitrogen in elderly patients with HFpEF:a retrospective cohort study

Running Title

Personalized Risk in HFpEF via Nutrition & BUN

Authers

Yanyan Li ,Hengyi Xue,XingmanFan,,Haitao Zhang,Yanjie Cao

Department of Cardiology,Air Force Medical Center,Air Force Medical University,PLA,100142 Beijing,China

Correspondence:kjzht@sina.com(Haitao Zhang) ;

18610089727@163.com（Yanjie Cao）

ABSTRACT

OBJECTIVE: To compare the prognostic value of six nutritional indices—BMI, HALP, TCBI, GNRI, CONUT, and PNI—for all-cause mortality in elderly patients with heart failure with preserved ejection fraction (HFpEF) and to identify an optimal BMI threshold and evaluate the modifying effect of BMI on blood urea nitrogen (BUN) as a predictor.

METHODS: This retrospective cohort study included hospitalized patients aged ≥65 years with HFpEF. Lasso-penalized Cox regression and XGBoost survival models with SHAP interpretability were used to assess each nutritional index's independent association with all-cause mortality, adjusted for demographics, comorbidities, medications, and laboratory parameters. Maximal log-rank statistics identified the optimal BMI cut-point for risk stratification. Decision curve analysis and Fine-Gray competing risk models were applied for clinical utility and cardiovascular mortality.

RESULTS: Among 228 elderly HFpEF patients (45.2% died during follow-up), BMI was the only nutritional index independently associated with all-cause mortality in Lasso-Cox regression (HR 0.93 per kg/m², 95% CI 0.88–0.98, P=0.009). The optimal BMI threshold was 24.46 kg/m², yielding a 59.6% relative risk reduction in the high-BMI group (HR 0.40, 95% CI 0.27–0.61, P<0.001). XGBoost identified BUN as the top predictor (mean SHAP 0.21) overall, but its importance differed markedly by BMI stratum: SHAP 0.18 in low-BMI vs. 0.05 in high-BMI patients. The BMI-based XGBoost model demonstrated modest validation performance (AUC 0.65) and achieved significant risk stratification only in the low-BMI subgroup (validation log-rank P=0.056), whereas stratification was not reproducible in the high-BMI subgroup. Decision curve analysis in the low-BMI subgroup showed that a BUN-only model achieved comparable net benefit to a full model combining BUN, age, neutrophil percentage, BNP and creatinine (standardized net benefit 0.79–0.87 vs. 0.81–0.89), indicating

that BUN alone may provide adequate clinical utility for risk stratification in this high-risk population.

CONCLUSION: In elderly HFpEF, the simple anthropometric measure BMI outperforms complex blood-derived nutritional indices for mortality prediction, with a threshold of approximately 24.5 kg/m² providing effective risk stratification; BUN's prognostic value is substantially stronger in patients with lower BMI, supporting BMI-stratified personalized prognostic models.

KEYWORDS: heart failure with preserved ejection fraction, nutritional assessment, body mass index, geriatric nutritional risk index, blood urea nitrogen, risk stratification

HIGHLIGHTS

- In elderly HFpEF, BMI independently predicts all-cause mortality while HALP, TCBI, GNRI, CONUT, and PNI do not;
- Optimal BMI cut-point of 24.46 kg/m² yields 60% relative risk reduction for all-cause death;
- Blood urea nitrogen prognostic value is 3.6-fold higher in low-BMI (≤24.46) vs. high-BMI patients;
- BMI-based XGBoost model effectively stratifies risk only in the low-BMI subgroup;
- Lasso-Cox and machine learning converge to identify BMI as the dominant nutritional index.

INTRODUCTION

HFpEF accounts for approximately half of all heart failure cases and is associated with substantial morbidity and mortality, particularly among the elderly [1]. The rising prevalence of HFpEF in aging populations, combined with a paucity of evidence-based therapies that consistently reduce mortality, underscores an urgent need for robust risk stratification tools to guide clinical decision-making. Although multiple pathophysiological pathways contribute to adverse outcomes in HFpEF, nutritional status has emerged as a critical modifiable determinant of prognosis, given its close interplay with inflammation, cachexia, and cardiorenal syndrome [2]. However, the optimal method for assessing nutritional risk in elderly HFpEF patients remains incompletely defined.

A large body of evidence has confirmed the so-called "obesity paradox" in heart failure, whereby higher body mass index (BMI) is paradoxically associated with better survival compared with normal or low BMI [2][3]. This pattern is also observed in HFpEF specifically, with meta-analyses suggesting a U-shaped relationship between BMI and all-cause mortality, with the lowest risk at moderately elevated BMI levels [1]. Nevertheless, the use of BMI alone as a nutritional index has been criticized for its inability to capture the

complexity of malnutrition, which includes deficits in protein stores, immune function, and micronutrient status. Consequently, several composite nutritional indices have been developed and validated in heart failure populations, including the Geriatric Nutritional Risk Index (GNRI) [4][5], Controlling Nutritional Status (CONUT) [6][7], Prognostic Nutritional Index (PNI) [7], and other markers such as the Triglyceride–Total Cholesterol–Body Weight Index (TCBI) and Hemoglobin–Albumin–Lymphocyte–Platelet Score (HALP). Systematic reviews have demonstrated that malnutrition defined by these multidimensional tools is associated with a 2- to 10-fold increase in mortality risk in chronic heart failure [2][8]. However, most existing studies have evaluated each index in isolation, and the relative predictive performance among these indices—especially in the specific context of elderly HFpEF—remains poorly characterized. Furthermore, prior meta-analyses emphasized that the prognostic significance of nutrition-associated markers in HFpEF is still unclear, highlighting the need for head-to-head comparisons within the same cohort [1].

Beyond specific nutritional indices, renal function parameters such as BUN have been identified as independent predictors of long-term mortality across diverse cardiovascular populations, including patients with acute myocardial infarction, atrial fibrillation, and critical illness. BUN elevation reflects not only glomerular filtration but also neurohormonal activation, protein catabolism, and volume status—all of which are particularly relevant in heart failure. Nonetheless, the interaction between BUN and nutritional status in elderly HFpEF patients has not been systematically examined, and whether the prognostic value of BUN differs across strata of body mass index is unknown.

Against this background, we conducted a comprehensive comparative analysis of six widely used nutritional indices—BMI, HALP, TCBI, GNRI, CONUT, and PNI—in a cohort of hospitalized elderly patients (≥65 years) with HFpEF. Using penalized Cox regression (LASSO) and machine learning survival models (XGBoost) with SHAP interpretability, we aimed to determine which index independently predicts all-cause mortality and to evaluate their incremental predictive value beyond traditional clinical covariates. Moreover, we sought to identify an optimal BMI threshold for risk stratification and to explore whether the prognostic utility of BUN varies according to BMI category. The findings of this study are intended to provide evidence-based guidance for selecting the most clinically useful nutritional assessment tool in this vulnerable population, and to uncover potential effect modifications that may inform personalized prognostic models.

METHODS

Study Population and Data Collection

This retrospective cohort study included elderly patients (≥65 years) with HFpEF admitted to the Air Force Medical Centre from January 2016 to December 2021. Patients with incomplete baseline data or loss to follow-up were excluded. Demographic information, clinical characteristics, laboratory parameters, medication history, and survival status were extracted from electronic medical records. All-cause mortality was the primary outcome, and

cardiovascular mortality was the secondary outcome. This retrospective study was approved by the Institutional Review Board of the Air Force Medical Centre (approval number:2024-71-PJ01) .Informed consent was waived by the IRB due to the retrospective nature of the study and the use of de-identified data.

Statistical Analysis

Baseline characteristics were compared between survivors and non-survivors using Student's t-test or Mann-Whitney U test for continuous variables and chi-square test or Fisher's exact test for categorical variables. Missing data were handled via complete-case analysis for the primary models; sensitivity analyses were performed using multiple imputation.

LASSO-Cox Regression for Variable Selection

To identify independent prognostic factors for all-cause mortality, least absolute shrinkage and selection operator (LASSO)-penalized Cox proportional hazards regression was applied. For each nutritional index (BMI, HALP, TCBI, GNRI, CONUT, and PNI), a separate LASSO-Cox model was fitted with the same set of covariates (age, sex, comorbidities, medications, and routine laboratory tests). The optimal penalty parameter λ was selected via 10-fold cross-validation using the minimum criterion (λ.min) and the one-standard-error rule (λ.1se). Variables with non-zero coefficients at λ.min were retained in the final model. Adjusted hazard ratios (HRs) with 95% confidence intervals (CIs) were calculated.

XGBoost-Cox Survival Models and SHAP Interpretation

To evaluate predictive performance, eXtreme Gradient Boosting (XGBoost)-Cox models were constructed using the same covariate set. The dataset was split into a training set (70%) and a validation set (30%). Model discrimination was assessed using time-dependent area under the receiver operating characteristic curve (AUC), and calibration was evaluated by comparing predicted risks with observed event rates. Variable importance was quantified using SHapley Additive exPlanations (SHAP) values. The mean absolute SHAP value of each predictor was reported to rank feature contributions.

Optimal Cut-point Determination

The maximally selected log-rank statistic implemented in the `maxstat` package of R was used to identify the optimal BMI cut-point for all-cause mortality risk stratification. The analysis scanned all candidate BMI values within the observed range, and the cut-point maximizing the standardized log-rank statistic was selected. Statistical significance was adjusted for multiple testing using the Lau94 method. Kaplan-Meier survival curves and univariable Cox regression were used to compare survival between the low-BMI and high-BMI groups.

Competing Risk Analysis

For cardiovascular mortality, cause-specific Cox proportional hazards regression with LASSO penalty was performed, and the Fine-Gray subdistribution hazard model was applied to account for the competing risk of non-cardiovascular death. Model selection was based on

10-fold cross-validated partial likelihood deviance. Interaction terms between BMI and other clinical variables (age, statin use, BNP) were explored using LASSO-penalized models.

Decision Curve Analysis

The clinical utility of the prognostic models was evaluated using decision curve analysis (DCA). Net benefit was calculated across a range of threshold probabilities for all-cause mortality. The analysis compared the full model (including BUN, age, neutrophil percentage, BNP, and creatinine) with the BUN-only model and the default strategies of "treat all" and "treat none".

Subgroup and Sensitivity Analyses

Subgroup analyses were performed by stratifying patients according to the optimal BMI cut-point. XGBoost-Cox models were rebuilt within each subgroup, and SHAP features were compared. Calibration, time-dependent AUC, and Kaplan-Meier curves were plotted for the training and validation sets. All analyses were conducted using R software with the `glmnet`, `xgboost`, `shapviz`, `maxstat`, `riskRegression`, and `dcurves` packages. A two-sided $p < 0.05$ was considered statistically significant.

RESULTS

Baseline characteristics

A total of 228 elderly patients (≥65 years) with HFpEF were included, with a median follow-up of approximately 2–3 years. Of these, 125 patients (54.8%) survived and 103 (45.2%) died from all causes. Baseline demographic, clinical, laboratory, and medication data stratified by survival status are summarized in Table 1.

Compared with survivors, non-survivors were significantly older (85.60 ± 7.50 vs. 80.26 ± 8.06 years, $p < 0.001$), had lower body weight (62.88 ± 12.17 vs. 68.10 ± 11.78 kg, $p = 0.001$) and lower BMI (22.80 ± 3.84 vs. 24.88 ± 3.46 kg/m², $p < 0.001$). Vital signs at admission did not differ between groups (all $p > 0.05$). Regarding cardiac function, non-survivors exhibited a slightly lower ejection fraction (55.65 ± 2.84 vs. 56.94 ± 4.34%, $p = 0.007$) and higher BNP levels (607.20 ± 765.80 vs. 367.91 ± 585.02 pg/ml, $p = 0.010$).

Among comorbidities, chronic kidney disease was more prevalent in non-survivors (38.83% vs. 20.80%, $p = 0.004$), whereas the frequencies of hypertension, atrial fibrillation, diabetes, COPD, stroke, hyperuricemia, and hyperlipidemia were comparable between groups (all $p > 0.05$). Regarding medications, statin use was markedly lower in non-survivors (45.63% vs. 75.20%, $p < 0.001$), as were antiplatelet agent (45.63% vs. 62.40%, $p = 0.016$) and anticoagulant use (7.77% vs. 18.40%, $p = 0.033$). No significant differences were observed for ACEI, ARB, beta-blockers, CCB, digoxin, or MRAs (all $p > 0.05$).

Several laboratory parameters differed significantly between groups. Non-survivors had higher neutrophil percentage (70.29 ± 14.32 vs. 65.52 ± 12.33%, $p = 0.008$), serum potassium (4.25 ± 0.63 vs. 4.04 ± 0.47 mmol/L, $p = 0.005$), creatinine (183.18 ± 179.33 vs. 129.30 ± 157.20 μmol/L, $p = 0.018$), and BUN (11.69 ± 8.14 vs. 8.62 ± 5.05 mmol/L, $p = 0.001$), together with a lower eGFR (63.11 ± 42.15 vs. 86.63 ± 53.12 ml/min/1.73 m²,

$p < 0.001$). Hemoglobin levels were significantly lower in non-survivors (109.83 ± 22.79 vs. 119.48 ± 20.26 g/L, $p < 0.001$). Total cholesterol was higher in the non-survivor group (4.08 ± 1.04 vs. 3.80 ± 0.98 mmol/L, $p = 0.039$), whereas LDL-cholesterol and HDL-cholesterol did not differ (both $p > 0.05$). Albumin levels showed a trend toward being lower in non-survivors, but the difference was not statistically significant (38.87 ± 4.44 vs. 39.88 ± 4.15 g/L, $p = 0.081$).

Regarding nutritional and immune-nutritional scores, non-survivors had significantly lower GNRI (97.15 ± 8.03 vs. 100.22 ± 6.77, $p = 0.002$) and higher CONUT scores (4.88 ± 1.33 vs. 4.37 ± 1.58, $p = 0.009$). The lymphocyte count score was also higher in non-survivors (1.58 ± 1.03 vs. 1.17 ± 1.09, $p = 0.004$). Other indices including HALP, TCBI, PNI, and albumin score did not differ significantly (all $p > 0.05$).

Comparative predictive performance of nutritional indices on all-cause mortality

Separate LASSO-regularised Cox regression models (α=1) were fitted for each nutritional index (BMI, HALP, TCBI, GNRI, CONUT and PNI) together with the same set of covariates including age, sex, comorbidities, medications, and routine laboratory tests. BMI was the only index that showed a statistically significant independent protective effect against all-cause mortality (HR=0.93, 95% CI 0.88–0.98, P=0.009). In contrast, HALP (coefficient shrunk to zero, HR=1.00, P=1.00), TCBI (coefficient shrunk to zero, HR=1.00, P=1.00), GNRI (HR=0.98, 95% CI 0.95–1.02, P=0.31), CONUT (coefficient shrunk to zero, HR=1.00, P=1.00) and PNI (HR=1.00, 95% CI 0.97–1.03, P=1.00) were not significantly associated with all-cause mortality. Age remained the strongest risk factor across all six models, with HRs ranging from 1.05 to 1.07 per year increase (all P<0.001). Statin use consistently showed a protective effect (HR range 0.61–0.70); it reached statistical significance in the PNI (HR=0.62, 95% CI 0.42–0.91, P=0.016) and TCBI (HR=0.61, 95% CI 0.41–0.89, P=0.010) models, and showed borderline significance in the BMI (HR=0.65, 95% CI 0.44–0.96, P=0.029), HALP (HR=0.69, 95% CI 0.46–1.03, P=0.068) and CONUT (HR=0.70, 95% CI 0.49–1.02, P=0.060) models (Table 2).

Model fitting and variable selection on all-cause mortality

The λ.min values (optimal penalty) ranged from 0.0238 (PNI) to 0.0726 (CONUT), and the number of selected non-zero coefficients varied from five (TCBI) to ten (HALP). The one-standard-error rule (λ.1se) selected more parsimonious models, retaining only one to five predictors. The cross-validated partial likelihood deviance at λ.min was similar across models (range 10.83–11.08), indicating comparable overall fit. For BMI specifically, λ.min was 0.0286, at which six covariates were retained. For HALP, λ.min was 0.0606 with 10 retained predictors; for TCBI, λ.min was 0.0261 with 5 retained predictors; For GNRI, λ.min was 0.0238 with six predictors retained; for PNI, λ.min was 0.0345 with five predictors retained.

LASSO-Cox findings for BMI on all-cause mortality

Further examination of the BMI model was performed. Figure 1 shows that λ.min was 0.0286, at which the partial likelihood deviance was 10.86 (SE 0.29) and six covariates retained non-zero coefficients. Figure 2 illustrates the shrinkage of coefficients as the penalty increased; BMI and statin maintained negative coefficients throughout, while age maintained

a positive coefficient. Figure 3 displays the adjusted HRs for all six selected variables. After multivariable adjustment, each 1 kg/m² increase in BMI was associated with a 7% lower risk of all-cause death (HR=0.93, 95% CI 0.88–0.98, P=0.009); statin use reduced risk by 35% (HR=0.65, 95% CI 0.44–0.96, P=0.029); and each 1-year increase in age raised risk by 6% (HR=1.06, 95% CI 1.04–1.09, P<0.001). Blood urea nitrogen (HR=1.02, 95% CI 0.99–1.05, P=0.24), neutrophil percentage (HR=1.01, 95% CI 0.99–1.03, P=0.26) and BNP (HR=1.00, 95% CI 0.9999–1.0006, P=0.19) were not significant. Interaction analysis did not identify any significant effect modification by BMI (all interaction P>0.05). Taken together, these findings indicate that in elderly HFpEF patients, the simple anthropometric measure BMI outperforms complex blood-derived nutritional indices in predicting all-cause mortality.

Predictive performance of nutritional indices in XGBoost-based models on all-cause mortality

We evaluated the prognostic ability of six nutritional indices—BMI, HALP, TCBI, GNRI, CONUT and PNI—using XGBoost survival models built on the same set of clinical covariates (age, sex, comorbidities, medications, and routine laboratory tests). Model performance was assessed by time-dependent AUC and the SHAP value of each index. Among the six indices, BMI achieved the highest validation AUC (mean = 0.65, range 0.62–0.72) together with a moderate SHAP contribution (0.08), whereas GNRI and CONUT showed comparable validation AUCs (0.70 and 0.69, respectively) but with lower SHAP values for GNRI (0.04) and CONUT (0.03). TCBI, HALP and PNI exhibited lower validation AUCs (0.68, 0.68 and 0.66, respectively) and negligible SHAP contributions (0.02, 0.03 and 0.02, respectively). The consistently higher training AUCs (0.95) across all models indicate strong internal discrimination, while the moderate validation AUCs highlight the need for further calibration.

Model discrimination and calibration across nutritional indices on all-cause mortality

The time-dependent AUC analysis revealed that the BMI model attained a mean training AUC of 0.95 and a mean validation AUC of 0.65; the HALP model achieved 0.95 and 0.68; the TCBI model 0.95 and 0.68; the GNRI model 0.95 and 0.70; the CONUT model 0.95 and 0.69; and the PNI model 0.95 and 0.66. Calibration curves generally showed progressive alignment between predicted risk and observed event rates, with perfect calibration in the highest risk bins (mean predicted risk >2.0 achieving 100% event rate) but under-prediction in the lowest risk bins (observed event rate 0% despite predicted risks around 0.30). These patterns were consistent across all six nutritional indices, suggesting that the XGBoost framework captures extreme risk well but tends to overestimate risk at the low end.

Feature importance and SHAP analysis for BMI on all-cause mortality

Because BMI was the only nutritional index with significant independent prognostic value in our previous LASSO-Cox analysis, we further examined its XGBoost model in detail. Figure 4 displays the SHAP summary plot, which ranks predictors by their mean absolute SHAP values. BUN was the most influential predictor (mean SHAP = 0.21), followed by age (0.15) and BNP (0.12). BMI itself contributed a mean SHAP of 0.08, placing it among the

top-five predictors together with statin use (0.07) and neutrophil percentage (0.06). Cardiovascular hemodynamic parameters (diastolic blood pressure = 0.04, eGFR = 0.03, ejection fraction = 0.03) showed moderate contributions, whereas most comorbidities and medications (e.g., hypertension, diabetes, ACEI, ARB) had negligible SHAP values (≤0.01). This hierarchy underscores the central roles of renal function, age, neurohormonal activation, and nutritional status in driving the model's predictions.

Time-dependent AUC and risk stratification for BMI on all-cause mortality

The discriminative ability of the BMI-based XGBoost model over time is shown in Figure 5. The training AUC remained consistently high, ranging from 0.95 at 579 days to 0.96 at 1094 days, whereas the validation AUC increased modestly from 0.62 at 579 days to 0.72 at 1094 days, with a mean validation AUC of 0.65. This pattern indicates that the model generalises reasonably well to unseen data, with performance improving over longer follow-up. Figure 6 presents Kaplan-Meier survival curves for patients dichotomised into high- and low-risk groups based on the XGBoost-derived risk score. In the training cohort (n=159, 85 events), the median risk score was 1.10, and the log-rank test yielded a highly significant separation ($\chi^2 \approx 60$, $p < 0.001$). In the validation cohort (n=69, 18 events), the median risk score was 1.12, but the log-rank chi-square statistic was only 0.1523 (df = 1), corresponding to a non-significant p-value of approximately 0.70, indicating that the survival difference between the two risk groups was not statistically reproducible in the validation set. This discrepancy highlights potential overfitting of the XGBoost model and suggests that the risk stratification derived from the training data may not generalise reliably to external cohorts. These results demonstrate that while the XGBoost model incorporating BMI achieves strong internal discrimination, its external validity remains limited. BMI itself contributes moderately to the predictive signature (mean SHAP = 0.08), but the lack of significant risk stratification in the validation cohort cautions against direct clinical application without further calibration.

Cardiovascular mortality

We applied Lasso-penalized Cox proportional hazards regression with competing risk framework to identify prognostic factors for cardiovascular mortality. Ten-fold cross-validation was performed on the complete cases (n=227) with 6 covariates including the primary variable of interest. The optimal regularization parameter was determined as $\lambda min = 0.0127$, which corresponded to the minimum partial likelihood deviance of 11.03 (SE = 0.23). At this optimal lambda, the model retained 3 non-zero coefficients, including BMI, statin use, and BNP levels, while the remaining covariates (age, neutrophil percentage, and BUN) were shrunk to zero, indicating their limited contribution to the predictive model under the elastic-net regularization framework (shown as Figure 7).

In the multivariate Lasso-penalized Cox model, body mass index demonstrated a non-significant protective trend toward cardiovascular mortality with a hazard ratio (HR) of 0.95 (95% CI: 0.85-1.08), although this association did not reach statistical significance (p = 0.45). The estimated coefficient was $\beta = -0.05$ (SE = 0.06), suggesting a potential inverse relationship between higher BMI and cardiovascular death in this elderly HFpEF cohort.

Among the other selected variables, statin use showed a protective effect with HR = 0.65 (95% CI: 0.27-1.59), though not statistically significant (p = 0.35). BNP levels demonstrated a marginal positive association with mortality (HR = 1.0004, 95% CI: 0.9998-1.0009, p = 0.23). Age, neutrophil percentage, and BUN were not selected in the final model, with coefficients shrunk to zero. The forest plot (Figure 8) visualizes the hazard ratios and 95% confidence intervals for all selected predictors, clearly demonstrating that none of the variables achieved statistical significance at the conventional $\alpha = 0.05$ level in this multivariate analysis.

To account for the competing risk of non-cardiovascular death, we performed Fine-Gray subdistribution hazard modeling in addition to the cause-specific Cox regression. The Fine-Gray model yielded consistent results with the Lasso Cox approach: BMI showed an HR of 0.95 (95% CI: 0.82-1.09), with a non-significant p-value of 0.47. The coefficient estimate was $\beta = -0.05$, very similar to the cause-specific Cox model ($\beta = -0.05$), indicating robust results across different analytical frameworks. The concordance between the two modeling approaches strengthens the validity of our findings, suggesting that BMI does not have a statistically significant independent association with cardiovascular mortality in this population, despite the observed protective trend.

We further explored potential interaction effects between BMI and other clinical variables (age, statin use, and BNP levels). The Lasso-penalized model with interaction terms identified an optimal λ of 0.0273, retaining one main effect (BMI) and one interaction term (BMI × Statin). However, the interaction term between BMI and statin use demonstrated a non-significant association (HR = 0.99, 95% CI: 0.96-1.01, p = 0.36), indicating no significant effect modification by statin therapy on the BMI-mortality relationship.

Optimal BMI cut-point for risk stratification

To identify a clinically applicable threshold for risk stratification, we performed maximally selected log-rank statistics (maxstat) analysis on the complete case cohort of 228 elderly HFpEF patients (103 all-cause deaths, event rate 45.2 %). The analysis scanned all candidate BMI cut-points within the observed range (12.49–33.58 kg/m², mean 23.94 ± 3.77 kg/m²). The optimal cut-point was determined at 24.46 kg/m², yielding a maximally standardized log-rank statistic of 4.39 (corrected $P = 0.00053$), which exceeded the significance boundary ($\alpha = 0.05$) after adjustment for multiple testing using the Lau94 method (Figure 9). At this cut-point, 121 patients (53.1 %) were classified into the low-BMI group (BMI ≤ 24.46 kg/m²) and 107 patients (46.9 %) into the high-BMI group (BMI > 24.46 kg/m²). The low-BMI group had a mean BMI of 21.14 ± 2.50 kg/m², experienced 70 events (57.9 % event rate) with a median follow-up of 1077 days (Q1 = 562, Q3 = 1667), whereas the high-BMI group had a mean BMI of 27.11 ± 2.08 kg/m², experienced 33 events (30.8 % event rate) with a longer median follow-up of 1477 days (Q1 = 796, Q3 = 2071). The Kaplan-Meier survival curves showed a markedly superior survival probability for the high-BMI group (log-rank $\chi^2 = 19.41$, $P < 0.001$). In the univariable Cox proportional hazards model with the low-BMI group as reference, the hazard ratio for all-cause death in the high-BMI group was 0.40 (95 % CI 0.27–0.61, $P < 0.001$), corresponding to a 59.6 % relative risk reduction. These findings indicate

that a BMI threshold of approximately 24.5 kg/m² effectively discriminates elderly HFpEF patients into low- and high-risk prognostic categories, supporting the obesity paradox in this population.

Subgroup Analysis Results by BMI Stratification

We conducted stratified analyses in elderly patients with HFpEF aged ≥65 years, dividing the cohort into two subgroups based on the optimal BMI cutpoint of 24.46 kg/m² identified by maximal log-rank statistic analysis: the low BMI group (BMI ≤ 24.46 kg/m², n=121) representing the high-risk subgroup, and the high BMI group (BMI > 24.46 kg/m², n=107) representing the low-risk subgroup. The XGBoost-based Cox proportional hazards model was trained on 70% of each subgroup and validated on the remaining 30%.

In the low BMI (high-risk) subgroup, the model achieved a training concordance index (C-index) of 0.94 and a validation C-index of 0.68, with 56 events in the training set and 13 events in the validation set during a median follow-up period. In the high BMI (low-risk) subgroup, the training C-index was 0.91, while the validation C-index was notably lower at 0.44, with 29 events in the training set and 5 events in the validation set. The substantially reduced validation performance in the high BMI group suggests potential model overfitting or heterogeneity in this subgroup, warranting cautious interpretation of the predictive variables.

Feature Importance and Key Predictor of BMI Stratification

SHAP (SHapley Additive exPlanations) analysis revealed distinct feature importance hierarchies between the two BMI subgroups. In the low BMI (high-risk) group, BUN emerged as the third most important predictor with a mean absolute SHAP value of 0.18, following only Age (0.45) and Neutrophil percentage (0.24). This finding suggests that renal function, as reflected by BUN, plays a crucial prognostic role in elderly HFpEF patients with lower BMI, who may represent a more frail population with compromised physiological reserve (Figure 10).

In stark contrast, within the high BMI (low-risk) subgroup, BUN ranked only 10th among predictors with a substantially attenuated SHAP value of 0.05. The top predictors in this group were Age (0.10), Creatinine (0.08), White blood cell count (0.08), BNP (0.07), and Ejection fraction (0.07). The diminished importance of BUN in the high BMI group indicates that the pathophysiological mechanisms linking renal function to mortality may differ according to body composition status, or that other factors become relatively more dominant in determining prognosis in overweight/obese patients.

Risk Stratification and Survival Curve Analysis

The XGBoost model successfully stratified patients into high-risk and low-risk groups in both subgroups based on the median risk score. In the low BMI group, the risk stratification yielded highly significant survival curve separation with an extremely significant log-rank

test ($p = 1.30 \times 10^{-21}$) in the training set and maintained significance in the validation set ($p = 5.59 \times 10^{-2}$). The high-risk group exhibited markedly higher cumulative mortality compared to the low-risk group, with the survival curves diverging early and remaining separated throughout the follow-up period.

In the high BMI group, while the training set demonstrated excellent discrimination (log-rank $p = 1.90 \times 10^{-13}$), the validation set showed no significant difference between risk groups ($p = 0.68$), indicating limited generalizability of the risk stratification model in this subgroup. This finding is consistent with the lower validation C-index observed and suggests that the complex interactions between clinical variables may not be adequately captured in the smaller high BMI validation cohort (n=33, with only 5 events).

Model Calibration and Time-Dependent AUC Analysis of BMI Stratification

Calibration analysis demonstrated excellent agreement between predicted risks and observed event rates in the high-risk strata for both groups. In the low BMI subgroup, the model showed perfect calibration in the highest risk bins, with observed event rates of 100% corresponding to predicted risks exceeding 1.0. The calibration curve in the high BMI group similarly showed strong concordance at the upper end of the risk spectrum, with event rates of 93.3% and 100% in the two highest risk bins.

Time-dependent AUC analysis revealed declining discriminative performance over follow-up time in both subgroups. In the low BMI group, the validation AUC decreased from 0.74 at 566 days to 0.62 at 1082 days, suggesting some temporal instability in predictive accuracy. The high BMI group exhibited more pronounced temporal degradation, with validation AUC values of 0.40, 0.45, and 0.41 at 601, 902, and 1146 days respectively, substantially below acceptable discrimination thresholds and reinforcing concerns about model generalizability in this subgroup.

Clinical Implications and Differential Role of BUN

The divergent importance of BUN between the two BMI-stratified subgroups represents a key finding with important clinical implications shown as Table 3. In elderly HFpEF patients with lower BMI (< 24.46 kg/m²), BUN serves as a powerful independent predictor of all-cause mortality, potentially reflecting the impact of cardiorenal syndrome and diminished nutritional reserve on outcomes. The strong association between BUN and mortality in this subgroup suggests that closer monitoring of renal function and aggressive management of factors contributing to prerenal azotemia may improve survival in this vulnerable population.

Conversely, in the high BMI group (≥ 24.46 kg/m²), BUN's predictive power was substantially attenuated, suggesting that the obesity paradox may operate through different pathophysiological pathways in HFpEF, or that the prognostic significance of renal dysfunction is confounded by the protective effects of higher body mass index. These findings underscore the importance of BMI-stratified risk assessment in elderly HFpEF patients and highlight the need for personalized prognostic models that account for body composition heterogeneity. Future studies should investigate the mechanisms underlying the

differential prognostic value of BUN across BMI strata and explore whether incorporating interaction terms or stratified modeling approaches improves predictive accuracy.

Decision Curve Analysis for All-Cause Mortality in BMI-Low HFpEF Patients

In this subgroup analysis of elderly patients with HFpEF aged ≥65 years, we conducted DCA to evaluate the clinical utility of BUN as the primary predictor of all-cause mortality, along with four auxiliary variables (age, neutrophil percentage, BNP, and creatinine). The DCA demonstrated that both the BUN-only model (baseline model) and the full model incorporating all five variables provided clinical net benefit across a wide range of threshold probabilities (0-40%). At threshold probabilities between 10% and 35%, the full model showed consistently higher net benefit compared to the BUN-only model, with the standardized net benefit ranging from 0.81 to 0.89 for the full model versus 0.79 to 0.87 for the baseline model. The BUN-only model exhibited net benefit above the "treat-all" and "treat-none" strategies across threshold ranges of 0.05-0.42, indicating its potential clinical utility for risk stratification in this population. The addition of age, neutrophil percentage, BNP, and creatinine to BUN marginally improved the net benefit, particularly at intermediate threshold probabilities (15-25%).

As illustrated in Figure 11, the decision curve analysis revealed that the full prediction model (BUN + Age + Neutrophil percentage + BNP + Creatinine) achieved the highest net benefit across most threshold probabilities, followed by the BUN-only model. Both models demonstrated superior clinical utility compared to the treat-all and treat-none strategies within the clinically relevant threshold range of 5-40%. The clinical impact analysis further confirmed that at a 20% threshold probability, approximately 82% of patients would be classified as high-risk by the full model, with a corresponding net benefit of 0.81. These findings suggest that incorporating the four auxiliary variables alongside BUN enhances the predictive performance for all-cause mortality in this elderly HFpEF cohort with low BMI, though the improvement over BUN alone is modest and may not justify the added complexity in clinical practice.

DISCUSSION

The observation that a simple anthropometric measure, body mass index (BMI), outperforms complex blood-derived nutritional indices in predicting all-cause mortality among elderly patients with HFpEF underscores a fundamental tension in contemporary risk stratification: multi-parameter scores are vulnerable to acute illness and renal dysfunction, whereas BMI may better capture long-term metabolic reserve and the protective effects of the obesity paradox [9,10]. In our LASSO-Cox models, each 1 kg/m² increase in BMI was associated with a 7% lower risk of all-cause death (HR 0.93, 95% CI 0.88–0.98, P = 0.009), whereas HALP, TCBI, GNRI, CONUT and PNI were either shrunk to zero or non-significant. This differential performance aligns with prior work showing that such indices often lose independence after multivariable adjustment [11,12], likely because their blood-based components—albumin, lymphocyte count, cholesterol—fluctuate with inflammation and congestion, whereas BMI remains relatively stable and integrates adiposity that may buffer catabolic stress [14]. In XGBoost models, BMI achieved the highest validation AUC (mean 0.65) among the six indices

and a SHAP contribution of 0.08, while GNRI and CONUT showed comparable AUCs but markedly lower SHAP values (0.04 and 0.03). We identified an optimal BMI cut-point of 24.46 kg/m² via maximally selected log-rank statistics (corrected P = 0.00053), below which the risk of death more than doubled (HR 0.40, 95% CI 0.27–0.61, P < 0.001). The apparent discrepancy between the hazard ratio for continuous BMI (HR 0.93 per 1 kg/m²) and that for BMI categorised at the 24.46 kg/m² cut-off (HR 0.40 for the high-BMI group vs. the low-BMI group) warrants clarification. This difference does not indicate statistical inconsistency, but rather reflects the non-linear (U-shaped or J-shaped) relationship between BMI and mortality in this elderly HFpEF population. The linear Cox model assumes a constant log-linear effect across the entire BMI spectrum, yielding an averaged estimate of 0.93. In contrast, the dichotomised comparison at the maximally selected cut-point captures the full contrast between the low-BMI and high-BMI groups, where the mean BMI values were 21.14 and 27.11 kg/m², respectively—spanning a 6-unit difference. The greater risk reduction observed in the categorised analysis (59.6%) suggests that the protective slope of BMI is steeper below the threshold than above it, consistent with the obesity paradox being most pronounced in the lower range of BMI. This non-linear pattern further supports the use of a threshold-based risk stratification approach in clinical practice, rather than assuming a uniform linear protective effect of BMI. The lack of significance for any blood-derived index in our LASSO-Cox framework may reflect the unique elderly, frail population (mean age >80 years) where acute-phase disturbances are common, and composite scores like HALP introduce collinearity with renal function and inflammation [16]. Of note, BMI's protective effect did not extend to cardiovascular mortality (HR 0.95, 95% CI 0.85–1.08, P = 0.45), suggesting its benefit is driven primarily by non-cardiovascular deaths—a pattern consistent with the obesity paradox being mediated through metabolic and immune reserve rather than direct cardiac protection [18–20].

The most striking finding of this study is that the prognostic relevance of BUN is fundamentally modified by BMI. In the overall LASSO-Cox model, BUN showed a non-significant HR of 1.02 (95% CI 0.99–1.05, P = 0.24), yet in the XGBoost framework it became the most influential predictor overall (mean SHAP 0.21), surpassing age (0.15) and BNP (0.12). This discordance—well documented in other clinical contexts [21,22]—reflects XGBoost's ability to capture non-linear threshold effects and high-order interactions that linear Cox models systematically miss, whereas LASSO may shrink BUN towards zero due to collinearity with creatinine or eGFR. More importantly, subgroup analysis revealed that BUN ranked third in SHAP importance in the low-BMI group (mean SHAP 0.18, behind age and neutrophil percentage), but dropped to tenth (SHAP 0.05) in the high-BMI group. Decision curve analysis in the low-BMI subgroup showed that a BUN-only model provided clinical net benefit across threshold probabilities of 5–42% (standardized net benefit 0.79–0.87), with only marginal improvement from adding age, neutrophil percentage, BNP and creatinine (0.81–0.89). This differential pattern suggests that in leaner, more frail patients, BUN—reflecting cardiorenal syndrome, prerenal azotemia, and catabolic stress—captures a dominant pathophysiological pathway, whereas in overweight patients, preserved metabolic reserve and distinct inflammatory profiles may attenuate its prognostic signal [23,24]. These findings are consonant with reports that low-BMI cardiac surgery patients exhibit higher BUN and greater renal vulnerability [56], reinforcing that low BMI may be a marker of underlying frailty and renal impairment.

The optimal BMI threshold of 24.46 kg/m² provided effective risk stratification (high-BMI group HR 0.40, 95% CI 0.27–0.61, P < 0.001), yet its utility is not uniform across analytical frameworks. While LASSO-Cox retained BMI as a significant predictor for all-cause mortality, XGBoost-based risk stratification incorporating BMI showed a validation AUC of only 0.65 and failed to achieve significant survival separation in the validation cohort (log-rank P ≈ 0.70), indicating overfitting.

Subgroup analyses further underscored this heterogeneity: the model's validation C-index was 0.68 in the low-BMI group but only 0.44 in the high-BMI group, with non-significant risk group separation in the latter (P = 0.68). These discrepancies suggest that the prognostic significance of BMI is not uniform and may be confounded by underlying frailty and renal function. While echocardiographic indices such as global longitudinal strain and TAPSE/PASP ratio may provide complementary one-year risk stratification [25], our threshold offers a readily accessible anthropometric tool. Nonetheless, the cut-point derived from a single-center cohort of 228 patients requires external validation before clinical adoption, and its predictive value for cardiovascular mortality remained non-significant, reinforcing the need for caution.

The failure of GNRI, CONUT, and PNI to independently predict mortality after multivariable adjustment—despite significant univariate differences—mirrors a persistent controversy in the literature [11,12,26]. In our study, non-survivors had significantly lower GNRI and higher CONUT, yet in LASSO-Cox models GNRI was non-significant (HR 0.98, P = 0.31) and CONUT, PNI, HALP, and TCBI had coefficients shrunk to zero. This attenuation likely arises from collinearity between their shared components (albumin, lymphocyte count, cholesterol) and inflammatory activation, renal dysfunction, and diuretic use—all captured by other covariates, a pattern also observed in septic ICU patients where nutritional scores lost significance after limited adjustment [27]. The divergent importance of BUN across BMI strata further implies that these indices may not reflect the same pathophysiology across the body composition spectrum; in leaner patients, prognostic signal may be driven by concurrent cardiorenal wasting, whereas in overweight patients, protective adipokine-mediated pathways may obscure the association. Future research should investigate whether serial trajectories, combination with novel biomarkers such as omentin [28], or disease-specific indices integrating mitochondrial dysfunction or fibroinflammatory remodeling [29] could outperform generic nutritional scores developed for surgical or oncologic populations.

The marked disparity between strong internal discrimination (training AUC ≈0.95) and poor external validation (validation AUC ≈0.65) in the XGBoost framework highlights overfitting to idiosyncratic features of the development cohort—a concern echoed across diverse clinical domains [31–33]. Strategies to mitigate this gap include nested cross-validation [34], diversity-guided stacking [35], hybrid feature-selection pipelines [35], and meta-learner training on out-of-fold predictions [36]; stacking ensembles have achieved very small overfitting gaps in other settings [37,38]. In our study, model complexity overwhelmed the limited event count (n=103), with the low-BMI subgroup yielding a validation C-index of 0.68 and the high-BMI subgroup dropping to 0.44. Direct comparisons with other ensemble approaches (e.g., CatBoost, LightGBM) that may have outperformed XGBoost in some contexts [39] were not performed and represent a critical evidence gap. Future work must adopt stricter feature pre-filtering and external validation in geographically diverse HFpEF cohorts.

The lack of statistical significance for statin use and BNP in the cardiovascular mortality model likely reflects insufficient statistical power rather than a true absence of biological effect. In our LASSO-penalized Cox model, both statin use (HR 0.65, 95% CI 0.27–1.59, P = 0.35) and BNP (HR 1.0004, 95% CI 0.9998–1.0009, P = 0.23) were retained but non-significant, contrasting with broader literature where statins reduce cardiovascular mortality by 26–31% [40,41] and BNP >100 pg/mL is associated with a nearly 5-fold increase in risk [42]. The wide confidence intervals strongly suggest insufficient power due to the small sample size and low cause-specific event rate, compounded by LASSO regularization. The divergence between all-cause and cardiovascular mortality findings also raises the possibility that competing risk of non-cardiovascular death—driven by frailty, infection, or renal failure—diluted the cause-specific signal, as supported by BUN being the most influential

predictor in XGBoost. Similarly, the variability in statin's protective effect across model specifications (significant in some LASSO-Cox models but with modest SHAP 0.07 in XGBoost) reflects differing handling of confounding and interactions; this pattern aligns with reports that statin benefits in HFpEF may be confounded by indication or effect modification [43], and our interaction analysis showed no significant BMI–statin interaction (HR 0.99, P = 0.36). Observational HFpEF studies should move beyond single-model inference and leverage causal inference methods to reduce residual confounding.

The growing emphasis on parsimonious risk stratification is fueled by repeated demonstrations that BUN consistently emerges as a top predictor across diverse clinical phenotypes [46–54]. In our study, BUN was the most influential feature in the full XGBoost model (SHAP 0.21), and decision curve analysis in the low-BMI subgroup revealed that a BUN-only model provided clinical net benefit across a threshold probability range of 5–42% (standardized net benefit 0.79–0.87), only marginally improved by adding four auxiliary variables (0.81–0.89). However, several nuances argue against premature practice change. First, BUN's performance was strikingly context-dependent: in the high-BMI subgroup, BUN dropped to tenth (SHAP 0.05) and the model's validation C-index fell to 0.44 with non-significant risk stratification, indicating that BUN's prognostic value is substantially attenuated in patients with higher BMI. Second, despite BUN's omnipresence in the literature, nearly all validated models employed multi-variable nomograms or ensembles, implying implicit recognition of the limitations of one-variable scores. Third, our DCA was performed only in the low-BMI subgroup; analogous analyses in the overall cohort and high-BMI stratum were not reported. The XGBoost model showed a validation AUC of only 0.65 and failed to achieve significant risk separation in the validation set, raising concerns that even the multi-variable model may overfit—a problem a simpler BUN-only model could potentially exacerbate. Future research should prospectively validate a streamlined two-variable risk score (BUN + a single BMI-stratified modifier) using dedicated decision-curve and calibration analyses across external cohorts, while also integrating competing-risk frameworks.

LIMITATIONS

This study has several limitations. First, the single-center retrospective design and modest sample size (n=228, 103 events) may limit statistical power and generalizability, particularly in subgroup analyses and the XGBoost validation set where the C-index dropped to 0.44 in the high-BMI group, and risk stratification in the validation cohort was non-significant (log-rank P≈0.70), underscoring potential overfitting. Second, residual confounding cannot be excluded; unmeasured factors such as sarcopenia, inflammatory markers, and detailed dietary intake were not available. Third, the nutritional indices were derived from admission laboratory values and may not reflect dynamic changes over time. Despite these constraints, the head-to-head comparative design and the use of both penalized regression and machine learning with SHAP interpretability provide robust internal comparisons. Future prospective, multicenter studies with larger, diverse populations and serial nutritional assessments are warranted to validate the differential prognostic utility of BUN across BMI strata and to confirm the optimal BMI threshold of 24.5 kg/m² identified here.

CONCLUSION

Among six nutritional indices evaluated in elderly patients with HFpEF, body mass index was the only independent predictor of all-cause mortality (HR 0.93 per kg/m², 95% CI 0.88–0.98), with an

optimal risk threshold of 24.46 kg/m² that yielded a 59.6% relative risk reduction in the high-BMI group, supporting the obesity paradox in this population. Notably, BUN emerged as the top contributor in machine learning models (mean SHAP 0.21) and its prognostic value was markedly accentuated in the low-BMI subgroup (SHAP 0.18) but attenuated in the high-BMI subgroup (SHAP 0.05), suggesting that BMI stratification redefines the predictive weight of renal markers. These findings support the use of simple BMI-based risk stratification in elderly HFpEF and highlight BUN as a particularly informative marker in underweight patients. Prospective validation in independent cohorts is needed before clinical implementation.

Declarations

Ethics approval and consent to participate

This retrospective study was approved by the Institutional Review Board of the Air Force Medical Centre (approval number: 2024-71-PJ01). Informed consent was waived by the IRB due to the retrospective nature of the study and the use of de-identified data.

Consent for publication

Not applicable.

Availability of data and materials

The datasets generated and/or analyzed during the current study are not publicly available due to patient confidentiality and institutional data protection policies but are available from the corresponding author upon reasonable request.

Competing interests

The authors declare that they have no competing interests.

Funding

This research received no specific grant from any funding agency in the public, commercial, or not-for-profit sectors.

REFERENCES

[1] Meng Ying, Zhang Zhengyi, Zhao Tong, Zhang Dekui. Prognostic Significance of Nutrition-Associated Markers in Heart Failure with Preserved Ejection Fraction: A Systematic Review and Meta-Analysis.. Arquivos brasileiros de cardiologia. 2023 120(5):e20220523. doi: 10.36660/abc.20220523. PMID: 37162076; PMCID: PMC10263396

[2] Wawrzeńczyk Anna, Anaszewicz Marzena, Wawrzeńczyk Adam, Budzyński Jacek. Clinical significance of nutritional status in patients with chronic heart failure-a systematic review.. Heart failure reviews. 2019 24(5):671-700. doi: 10.1007/s10741-019-09793-2. PMID: 31016426

[3] Lin Gen-Min, Li Yi-Hwei, Yin Wei-Hsian, Wu Yen-Wen, Chu Pao-Hsien, Wu Chih-Cheng, et al.. The Obesity-Mortality Paradox in Patients With Heart Failure in Taiwan and a Collaborative Meta-Analysis for East Asian Patients.. The American journal of cardiology. 2016 118(7):1011-8. doi: 10.1016/j.amjcard.2016.06.056. PMID: 27521221

[4] Dong Chao-Hui, Chen Si-Yu, Zeng Hong-Lian, Yang Bo, Pan Jia. Geriatric nutritional risk index predicts all-cause mortality in patients with heart failure: A systematic review and meta-analysis.. Clinics (Sao Paulo, Brazil). 2021 76:e2258. doi: 10.6061/clinics/2021/e2258. PMID: 33787674; PMCID: PMC7955148

[5] Li Hengdong, Cen Kaidong, Sun Weifeng, Feng Beili. Prognostic value of geriatric nutritional risk index in elderly patients with heart failure: a meta-analysis.. Aging clinical and experimental research. 2021 33(6):1477-1486. doi: 10.1007/s40520-020-01656-3. PMID: 32766928

[6] Osório Amanda Farias, Ribeiro Édina Caroline Ternus, Parahiba Suena Medeiros, Forte Gabriele Carra, Clausell Nadine Oliveira, Souza Gabriela Corrêa. Prognostic value of nutritional screening tools in hospitalized patients with decompensated heart failure: A systematic review and meta-analysis.. Nutrition research (New York, N.Y.). 2023 120:1-19. doi: 10.1016/j.nutres.2023.09.009. PMID: 37871448

[7] Hu Yule, Yang Haojie, Zhou Yanjun, Liu Xin, Zou Changhong, Ji Shiming, et al.. Prediction of all-cause mortality with malnutrition assessed by nutritional screening and assessment tools in patients with heart failure：a systematic review.. Nutrition, metabolism, and cardiovascular diseases : NMCD. 2022 32(6):1361-1374. doi: 10.1016/j.numecd.2022.03.009. PMID: 35346547

[8] Knobloch Ingrid da Silveira, Zucatti Kelly Pozzer, de Carvalho Bruna Zardo Oliveira, da Costa-Pereira Jarson P, Hartmann Alicia Sommer, Razzera Elisa Loch, et al.. Prevalence of malnutrition and its association with outcomes in heart failure: A systematic review and meta-analysis.. Nutrition (Burbank, Los Angeles County, Calif.). 2025 140:112913. doi: 10.1016/j.nut.2025.112913. PMID: 40886401

[9] Shi Xiuli, Wang Xuefeng, Li Yixuan, Luo Hao, Li Yihang, Lai Na, et al.. The causal role of genetically predicted obesity-related traits in heart failure: systematic review and meta-analysis of Mendelian randomization studies.. Frontiers in cardiovascular medicine. 2026 13:1798689. doi: 10.3389/fcvm.2026.1798689. PMID: 42039359; PMCID: PMC13105879

[10] Yadav Ashish, Manandhar Sareeta, Kloster Alex, Aradhyula Vaishnavi, Maddipati Krishna Rao, Moukarbel George V, et al.. Obesity is associated with distinct oxylipins in heart failure with preserved ejection fraction.. Metabolomics : Official journal of the Metabolomic Society. 2026 22(3). doi: 10.1007/s11306-026-02449-x. PMID: 42115484; PMCID: PMC13160996

[11] Chen Ying, Zheng Hui, He Yu. Prognostic significance of controlling nutritional status in older adults with heart failure with preserved ejection fraction: a prospective comparative study with other objective nutritional indices.. Aging clinical and experimental research. 2023 35(6):1305-1315. doi: 10.1007/s40520-023-02395-x. PMID: 37005959; PMCID: PMC10200784

[12] Fan Xingman, He Qiongyi, Zhang Kaijie, Lan Xiaohua, Li Yanyan, Zhang Haitao. Comparison of the Value of Four Objective Nutritional Indices in Assessing the Long-Term Prognosis of Elderly

Patients with Heart Failure with Preserved Ejection Fraction.. Reviews in cardiovascular medicine. 2024 25(6):201. doi: 10.31083/j.rcm2506201. PMID: 39076344; PMCID: PMC11270056

[13] Seo Masahiro, Yamada Takahisa, Tamaki Shunsuke, Hikoso Shungo, Yasumura Yoshio, Higuchi Yoshiharu, et al.. Prognostic Significance of Serum Cholinesterase Level in Patients With Acute Decompensated Heart Failure With Preserved Ejection Fraction: Insights From the PURSUIT-HFpEF Registry.. Journal of the American Heart Association. 2020 9(1):e014100. doi: 10.1161/JAHA.119.014100. PMID: 31847660; PMCID: PMC6988145

[14] Draghici Anamaria, Dan Gheorghe-Andrei. Clinical Prognostic Scoring Systems in Heart Failure with Preserved Ejection Fraction: An Integrative Review of Risk Prediction Models.. Romanian journal of internal medicine = Revue roumaine de medecine interne. 2026. doi: 10.2478/rjim-2026-0002. PMID: 41770523

[15] Czapla Michał, Kwaśny Adrian, Uchmanowicz Izabella, Pietrzykowski Łukasz, Lee Christopher S, Kosowski Wojciech, et al.. Sex differences in the association between nutritional status and in-hospital mortality in HFpEF patients.. ESC heart failure. 2025 12(4):2499-2506. doi: 10.1002/ehf2.15332. PMID: 40396460; PMCID: PMC12287804

[16] Ucdal Mete, Ekingen Evren, Yurtsever Karya, Celik Melike Elif, Kuru Saniye Beyza. Cardiometabolic indices as predictors of clinical outcomes in palliative care patients.. PloS one. 2026 21(5):e0338562. doi: 10.1371/journal.pone.0338562. PMID: 42102173; PMCID: PMC13155664

[17] Wilk Michał, Kotwica Tomasz, Zymliński Robert, Gajewski Piotr. Strengths and limitations of HFpEF probability scores in the era of precision medicine.. Frontiers in medicine. 2026 13:1799451. doi: 10.3389/fmed.2026.1799451. PMID: 42023091; PMCID: PMC13095507

[18] Garin Nicolas, Carballo David, Dash Jonathan, Stirnemann Jérôme, Reny Jean-Luc, Vuilleumier Nicolas, et al.. Overweight and obesity association with mortality in patients with heart failure and reduced or preserved ejection fraction-a cohort study.. PloS one. 2026 21(2):e0341606. doi: 10.1371/journal.pone.0341606. PMID: 41632717; PMCID: PMC12867239

[19] Tannous Lana, Tated Ritu, Ramesh Jaishkar, Joshi Dhruvi K, Jain Hritvik, Agrawal Siddharth P. The Obesity Paradox in Heart Failure With Preserved Ejection Fraction: Untangling Body Composition, Inflammation, and Outcomes.. Cardiology in review. 2025. doi: 10.1097/CRD.0000000000001106. PMID: 41198097

[20] Alebna Pamela L, Martey Sarah, Mehta Anurag, Lavie Carl J, Carbone Salvatore. The Treatment of Obesity in the Context of the Obesity Paradox in Patients with Heart Failure: A Narrative Review.. Current cardiology reports. 2025 28(1):4. doi: 10.1007/s11886-025-02333-5. PMID: 41400711; PMCID: PMC12708749

[21] Li Yunhang, Bu Xiaoli, Geng Zhengguang, Dai Ninan, Fu Bao, Deng Renli, et al.. Interpretable machine learning for predicting in-hospital mortality in COPD ICU patients: a rigorous validation across time and geography.. Respiratory research. 2026. doi: 10.1186/s12931-026-03702-6. PMID: 42121158

[22] Sun Manxiang, Wang Ling, Yang Jing. A machine learning-based prediction model for in-hospital mortality in ICU patients with acute rhinosinusitis: A multi-database study using SHAP interpretability.. Medicine. 2026 105(17):e48376. doi: 10.1097/MD.0000000000048376. PMID: 42071837; PMCID: PMC13124349

[23] Soerarso Rarsari, Hasanah Dian Yaniarti, Yonas Emir, Pratama Ahmad Pandu, Raharjo Sunu Budhi, Siswanto Bambang Budi, et al.. Factors Predicting Diuretic Resistance in Patients With Acute Decompensated Heart Failure.. Journal of clinical medicine research. 2026 18(4):270-280. doi: 10.14740/jocmr6391. PMID: 42016335; PMCID: PMC13094107

[24] Zhang Jianhui, Zhang Xiaoyi, Kuai Zheng, Zou Yunzeng, Yuan Jie. Association between Tubular Injury Biomarkers and Early Renal Injury in Hypertensive Patients.. International heart journal. 2026 67(2):156-163. doi: 10.1536/ihj.25-515. PMID: 41922284

[25] Senthamil Selvan Pradesh Kumar, Pandiyan Pradeepha Rani, Prasanth Ram, Rajendran Revathi, Subramanian Lakshmi Uma Kiruthika, Irfan Shahul. Echocardiographic Predictors of Readmission and Mortality in Elderly Patients With Heart Failure and Preserved Ejection Fraction: A Prospective Observational Study.. Cureus. 2025 17(9):e92312. doi: 10.7759/cureus.92312. PMID: 41111697; PMCID: PMC12529852

[26] Sonaglioni Andrea, Lonati Chiara, Donzelli Andrea, Napoli Federico, Nicolosi Gian Luigi, Baravelli Massimo, et al.. Prognostic Role of Immunonutritional Indices in Elderly Patients with HFpEF: Long-Term Follow-Up of the CONUT, PNI, and CALLy Scores.. Journal of clinical medicine. 2026 15(9). doi: 10.3390/jcm15093245. PMID: 42122988; PMCID: PMC13163737

[27] Novac Marius Bogdan, Gorecki Gabriel-Petre, Pătru Alin, Dijmărescu Anda Lorena, Hădăreanu Diana-Ruxandra, Assani Mohamed-Zakaria, et al.. Prognostic Value of Nutritional Risk Scores in Septic ICU Patients: A Survival Analysis Using mNUTRIC, PNI, and CONUT.. Diagnostics (Basel, Switzerland). 2026 16(8). doi: 10.3390/diagnostics16081193. PMID: 42072818; PMCID: PMC13114300

[28] Currò Diego, Vergani Edoardo, Nicolazzi Maria Anna, Favuzzi Angela Maria Rita, Angelini Flavia, Mancini Antonio, et al.. Circulating Omentin Levels in Heart Failure: A Case-Control Study.. International journal of molecular sciences. 2026 27(9). doi: 10.3390/ijms27093998. PMID: 42123575; PMCID: PMC13164156

[29] Ganguly Souradipta, Gunes Betul, Gu Yusu, Suarez Jorge, Gupta Gautam, Ishizuka Kei, et al.. A Translational Model of MASLD-Associated HFpEF Defines Mitochondrial Dysfunction and Cardiac Plasticity During Disease Progression and Regression.. bioRxiv : the preprint server for biology. 2026. doi: 10.64898/2026.02.26.708088. PMID: 42124725; PMCID: PMC13160009

[30] Günther Oliver P, Sherwood Karen R, Fenninger Franz, Balshaw Robert F, Scherer Andreas, Hollander Zsuzsanna, et al.. Bioinformatics strategies and biomarker refinement using high-throughput transcriptome data in transplantation.. Frontiers in bioinformatics. 2026 6:1677453. doi: 10.3389/fbinf.2026.1677453. PMID: 42028568; PMCID: PMC13099910

[31] Mao Leiming, He Ruiqi, Zhang Shike, Ge Yongqian, Xu Entong, Chen Yalan, et al.. Impact of the Interaction Between Screen Time and Activity Interests on Adolescent Depression Risk: Construction of a Predictive Model Based on Machine Learning.. Actas espanolas de psiquiatria. 2026 54(2):500-515. doi: 10.62641/aep.v54i2.2068. PMID: 42023462

[32] Wang Jinyu, Zhang Xinran, Li Sheng. Development and validation of a machine learning model for predicting occupational stress among primary and secondary school teachers.. Frontiers in public health. 2026 14:1767113. doi: 10.3389/fpubh.2026.1767113. PMID: 42027941; PMCID: PMC13101654

[33] Faruk Omar. Climate-Driven Advanced Machine Learning Approach for Dengue Incidence Forecasting in Bangladesh.. Health science reports. 2026 9(4):e72207. doi: 10.1002/hsr2.72207. PMID: 42005651; PMCID: PMC13087637

[34] Petit Pascal, Nübel Jonathan, Walter Marie Josephine, Butter Christian, Heinze Martin, Ignatyev Yuriy, et al.. Telemedicine adoption in cardiology: Determinants and predictors identified using Bayesian Model Averaging and Machine Learning.. PLOS digital health. 2026 5(4):e0001359. doi: 10.1371/journal.pdig.0001359. PMID: 42008527; PMCID: PMC13095100

[35] Mohtasham Farideh, Hashemi Nazari Seyed Saeed, Pourhoseingholi Mohamad Amin, Kavousi Kaveh, Zali Mohammad Reza. Hybrid feature-selection and diversity-guided stacking framework for interpretable ensemble learning: Application to COVID-19 mortality prediction.. PloS one. 2026 21(4):e0341198. doi: 10.1371/journal.pone.0341198. PMID: 41996322; PMCID: PMC13089710

[36] Baral Sumati, Satpathy Suneeta, Satpathy Rabi Narayan, Kumar Baral Ajit. Comparative Evaluation of Ensemble Machine Learning Approaches for Heart Disease Prediction.. Journal of visualized experiments : JoVE. 2026. doi: 10.3791/70124. PMID: 42044068

[37] Thangaganesan Chandradevi Sabareeswari, Ramachandran Dhanagopal. SAT-inspired feature engineering with stacking ensemble learning for fault detection in digital logic circuits.. Scientific reports. 2026. doi: 10.1038/s41598-026-50142-9. PMID: 42082575

[38] Teng Xiaoyan, Qiao Ji, Xue Yang, Wei Li, Ji Xiaozhong, Du Yuzhen. A multiparameter model (OsteoSC-M3) for early detection and risk stratification of osteoporosis in women: a multicentre cohort study in China.. EClinicalMedicine. 2026 95:103902. doi: 10.1016/j.eclinm.2026.103902. PMID: 42016607; PMCID: PMC13092471

[39] Yu Hang, Xiao Tingwei, Li Yingying, Li Zhuyin, Liu Jiaxi, Zhao Hongguo, et al.. Analysis and application of a machine learning-based assisted diagnosis method for myofascial pelvic pain syndrome.. Frontiers in medicine. 2026 13:1627891. doi: 10.3389/fmed.2026.1627891. PMID: 42058414; PMCID: PMC13121126

[40] Yuan Cheng, Ge Yuguo, Ge Wenqi, Wang Huaxue, Deng Ximing, Chen Jinmeng, et al.. Effect of Statin Use on Mortality in Individuals With Cardiovascular-Kidney-Metabolic Syndrome: A Retrospective Propensity Score-Matched Cohort Study.. Cardiovascular therapeutics. 2026 2026(1):e7480081. doi: 10.1155/cdr/7480081. PMID: 41918270; PMCID: PMC13140241

[41] Mirhosseini Seyed Alireza, Azami Pouria, Mirzaei Alisina, Zooravar Diar, Yaghoobi Narges, Arman Ali, et al.. The Effectiveness of Polypills for Primary and Secondary Prevention of Major Adverse Cardiovascular Events: A Systematic Review and Meta-Analysis.. Cardiology in review. 2026. doi: 10.1097/CRD.0000000000001251. PMID: 41952094

[42] Farhan Muhammad, Patel Tirath, Ahmed Shahbaz Ahmed Sheikh Bilal, Abdelrazek Arwa Ossama, Aliefiyanto Rafi, Khattak Muhammad Yahya, et al.. Diabetic Foot Ulcer as an Independent Risk Factor for Cardiovascular Mortality: A Systematic Review and Meta-Analysis With Qualitative Synthesis of Cardiac Biomarker Evidence.. Cureus. 2026 18(4):e106672. doi: 10.7759/cureus.106672. PMID: 42110017; PMCID: PMC13155703

[43] Al-Jarallah Mohammed, Rajan Rajesh, Dashti Raja, Bulbanat Bassam, Ridha Mustafa, Sulaiman Kadhim, et al.. Impact of Statin Therapy on Mortality and Rehospitalization in Acute Heart Failure Patients Stratified by Ejection Fraction: Insights from the Gulf CARE Registry.. Current vascular pharmacology. 2025. doi: 10.2174/0115701611311671250416054455. PMID: 40325528

[44] Urbanowicz Tomasz K, Gabriel Katarzyna, Spasenenko Ievgen, Krasińska-Płachta Aleksandra, Banaszkiewicz Marta, Filipiak Krzysztof J, et al.. The possible modulatory impact of high-dose statin therapy on carotid intima-media thickness: a preliminary study.. Postepy w kardiologii interwencyjnej = Advances in interventional cardiology. 2024 20(4):413-419. doi: 10.5114/aic.2024.145183. PMID: 39897017; PMCID: PMC11783262

[45] Urbanowicz Tomasz, Spasenenko Ievgen, Banaszkiewicz Marta, Olasińska-Wiśniewska Anna, Krasińska-Płachta Aleksandra, Tykarski Andrzej, et al.. The Possible Role of Rosuvastatin Therapy in HFpEF Patients-A Preliminary Report.. Diagnostics (Basel, Switzerland). 2024 14(22). doi: 10.3390/diagnostics14222579. PMID: 39594245; PMCID: PMC11592476

[46] He Lu, Zhang Mengyu, Wang Xuanxuan, Wang Tian, Wang Peng. Machine learning-based prediction of diabetic retinopathy using clinlabomics: a multi-center study.. BMC medical informatics and decision making. 2026. doi: 10.1186/s12911-026-03524-y. PMID: 42116016

[47] Zeng Yongjun, Wang Jinlin, Lin Kun, Ao Lu, Zhu Chenggong, Yi Qiang, et al.. Machine learning-based prediction of NAFLD in patients with type 2 diabetes using routine clinical and biochemical indicators.. Frontiers in endocrinology. 2026 17:1761846. doi: 10.3389/fendo.2026.1761846. PMID: 42051460; PMCID: PMC13111042

[48] Ge Ya-Nan, Ouyang Yu-Man, Li Qian-Qian, Huang Jie, Li Dai, Wang Chang-Li, et al.. Preoperative frailty for predicting in-hospital mortality in patients after cardiac surgery: an interpretable Machine learning model based on a retrospective multicenter cohort study.. International journal of medical informatics. 2026 215:106437. doi: 10.1016/j.ijmedinf.2026.106437. PMID: 42008965

[49] Wu Weiqin, Han Xiang, Yan Zhuan, Gao Lili, Sun Qingsong. A multimodal predictive model incorporating transcriptomic-guided blood biomarkers and clinical variables for sepsis-associated acute kidney injury.. Renal failure. 2026 48(1):2641853. doi: 10.1080/0886022X.2026.2641853. PMID: 41937676; PMCID: PMC13055026

[50] Ying Yiling, Yuan Xiangshu, Zhang Xian, Wang Guangdong, Gao Lang, Ge Yuanshuo, et al.. Creatinine-to-albumin ratio for early ICU-course (first 24 hours) risk stratification of mortality in critically ill patients with gastrointestinal bleeding: A retrospective cohort study.. Science progress. 2026 109(2):368504261441729. doi: 10.1177/00368504261441729. PMID: 41934121; PMCID: PMC13051087

[51] Zhu Jichong, Huang Chengqian, Lin Yang, Chen Tianyou, Ren Lei, Chen Jiarui, et al.. A multicenter explainable machine learning analysis of autoimmune disease comorbidity in ankylosing spondylitis.. Frontiers in immunology. 2026 17:1775877. doi: 10.3389/fimmu.2026.1775877. PMID: 41836410; PMCID: PMC12979442

[52] Zhang Yue, Wang Chenguang, Chai Yanfen. Development and validation of a prediction model for predicting invasive Klebsiella pneumoniae liver abscess syndrome in patients with pyogenic liver abscess.. BMC infectious diseases. 2026 26(1). doi: 10.1186/s12879-026-12727-7. PMID: 41667989; PMCID: PMC12990508

[53] Chai Ya-Ge, Gou Yi, Cong Yun, Li Dan-Dan, Yang Jian-Zhong, Peng Peng. Development and Validation of a Risk Prediction Model for New-Onset Atrial Fibrillation in Sepsis.. International journal of general medicine. 2025 18:7471-7482. doi: 10.2147/IJGM.S567490. PMID: 41404023; PMCID: PMC12704190

[54] He Mengwei, Zhang Xiang, Huo Weixue, Qu Jin, Wang Sen, Zeng Zhaoxiang, et al.. Predicting ICU mortality in patients with abdominal aortic aneurysm: a nomogram based on MIMIC-IV and eICU-CRD.. International journal of medical sciences. 2026 23(1):146-160. doi: 10.7150/ijms.116265. PMID: 41399368; PMCID: PMC12702021

[55] Komukai Kimiaki, Minai Kosuke, Arase Satoshi, Ogawa Takayuki, Nakane Tokiko, Nagoshi Tomohisa, et al.. Impact of body mass index on clinical outcome in patients hospitalized with congestive heart failure.. Circulation journal : official journal of the Japanese Circulation Society. 2012 76(1):145-51. doi: 10.1253/circj.cj-11-0727. PMID: 22094909

[56] Chang Chiu-Hsia, Lee Fan-Yen, Wang Chin-Chou, Chen Ying-Ni, Chen Hsin-Chu, Hung Huei-Ling, et al.. An obesity paradox of Asian body mass index after cardiac surgery: arterial oxygenations in duration of mechanic ventilation.. TheScientificWorldJournal. 2013 2013:426097. doi: 10.1155/2013/426097. PMID: 24163622; PMCID: PMC3791635

[57] Gameil Mohammed Ali, Marzouk Rehab Elsayed, El-Sebaie Ahmed Hassan, Eldeeb Ahmed Ahmed Ahmed. Influence of sodium-glucose Co-transporter 2 inhibitors on clinical and biochemical markers of dehydration during the Holy Ramadan.. Diabetes & metabolic syndrome. 2022 16(9):102606. doi: 10.1016/j.dsx.2022.102606. PMID: 36063675

[58] Alyami Hanan, Alshuweishi Fahd A, Baghdadi Nadiah A, Al-Sharafa Meshal Marzoog, Jaber Alqahtani Ali, Alshuweishi Yazeed. Declining eGFR and Uremia Are Associated with Remnant Cholesterol Accumulation and Reduced HDL-C in Non-Dialysis Chronic Kidney Disease.. Journal of clinical medicine. 2026 15(8). doi: 10.3390/jcm15082918. PMID: 42074721; PMCID: PMC13116661

[59] Soltani Rasool, Khorvash Farzin, Meidani Mohsen, Badri Shirinsadat, Alaei Sajedeh, Taheri Shahram. Vitamin E in the prevention of vancomycin-induced nephrotoxicity.. Research in pharmaceutical sciences. 2020 15(2):137-143. doi: 10.4103/1735-5362.283813. PMID: 32582353; PMCID: PMC7306246

[60] Yuyen Thassayu, Intusut Monnanee, Phothikun Natsuda, Thanakiattiwibun Chayanan, Thitisakulchai Poungkaew, Tanvijit Phakamas. A pragmatic approach to identifying postextubation dysphagia in critically ill surgical patients using the water swallow test.. Scientific reports. 2026 16(1):5253. doi: 10.1038/s41598-026-35533-2. PMID: 41535342; PMCID: PMC12881625

[61] Wu Dan, Qin Haidong, Zhou Suming. The diagnostic and prognostic value of sTM, t-PAIC, and NLRP3 in ICU patients with sepsis.. BMC infectious diseases. 2026. doi: 10.1186/s12879-026-13466-5. PMID: 42129677

[62] El Shebini Salwa M, Youness Eman R, Ahmed Nihad H, Orban Hisham A, Mohamed Rehab A, Moaty Maha I A. Effect of nutritional intervention on interleukin-18 and alpha-2-macroglobulin in women with obesity and metabolic dysfunction-associated fatty liver disease: a prospective cohort study.. Journal of health, population, and nutrition. 2026 45(1). doi: 10.1186/s41043-026-01324-8. PMID: 42116229; PMCID: PMC13159282

[63] Hou Xiaoxiao, Chen Ying, Wang Qi, Sun Yuqi, Tong Shan, Liu Kai. Association between the cumulative average triglyceride glucose-BMI and hypertension incidence among the middle-aged and older population: a prospective nationwide cohort study in China.. Journal of hypertension. 2026. doi: 10.1097/HJH.0000000000004312. PMID: 42132510

[64] Pant Abhishek, Anjankar Ashish. Predictive Utility of Atherogenic Index of Plasma in Carcinoma Breast Cases in Correlation with Oxidative Stress, Immuno-biomarkers and Body Mass Index.. The

Nigerian postgraduate medical journal. 2026 33(3):353-357. doi: 10.4103/npmj.npmj_279_25. PMID: 42085057

FIGURE LEGENDS

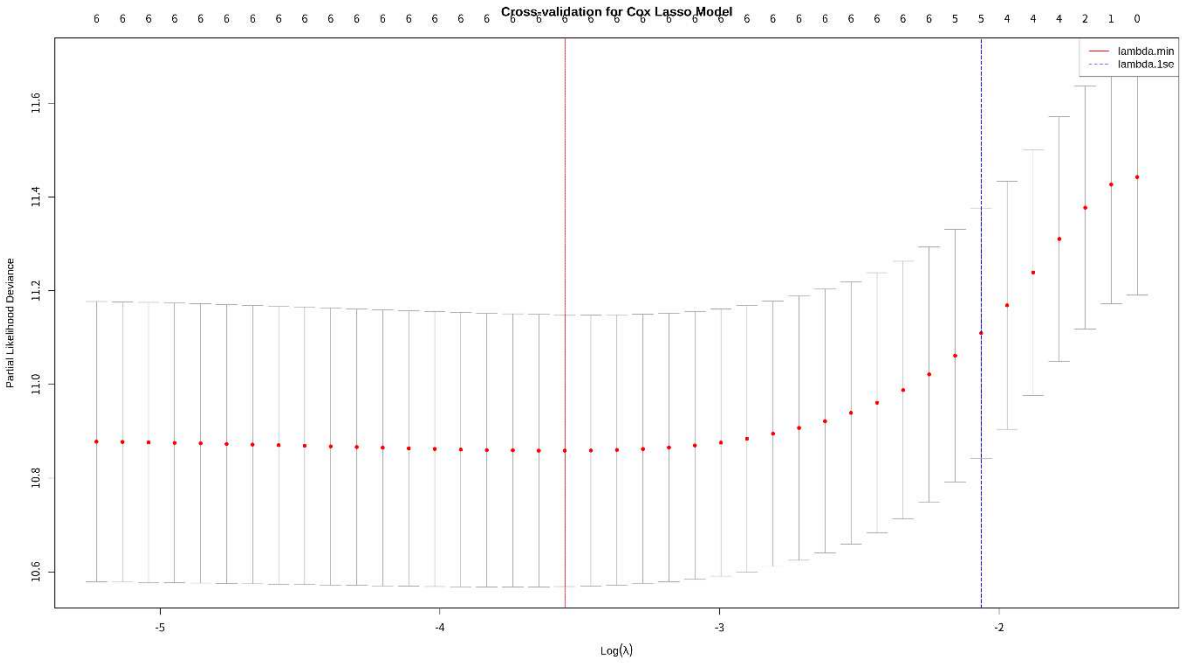


Figure 1. Cross-validation curve for the BMI LASSO-Cox model.

The vertical axis shows partial likelihood deviance, the horizontal axis log(λ). The red dashed line marks λ.min (0.0286), and the blue dashed line marks λ.1se (0.1269). Error bars represent ±1 standard error.

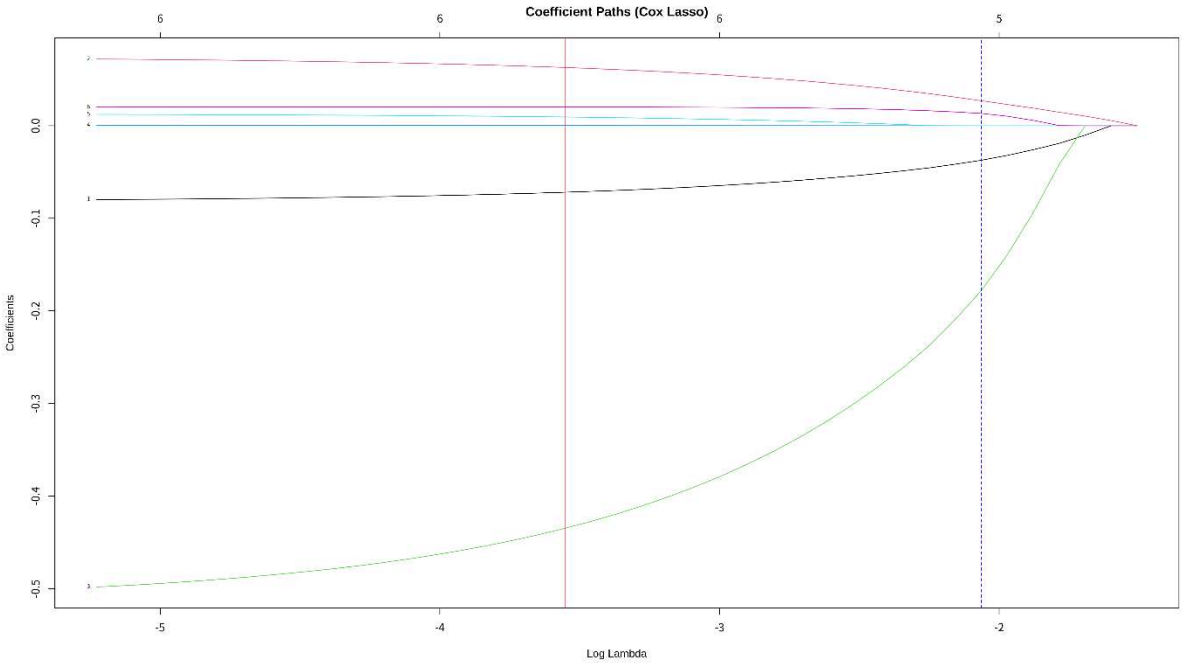


Figure 2. Coefficient path plot for the BMI LASSO-Cox model.

Each line represents the trajectory of a coefficient as the penalty λ increases. Positive coefficients increase hazard, negative coefficients decrease hazard. The vertical red line is at λ.min.

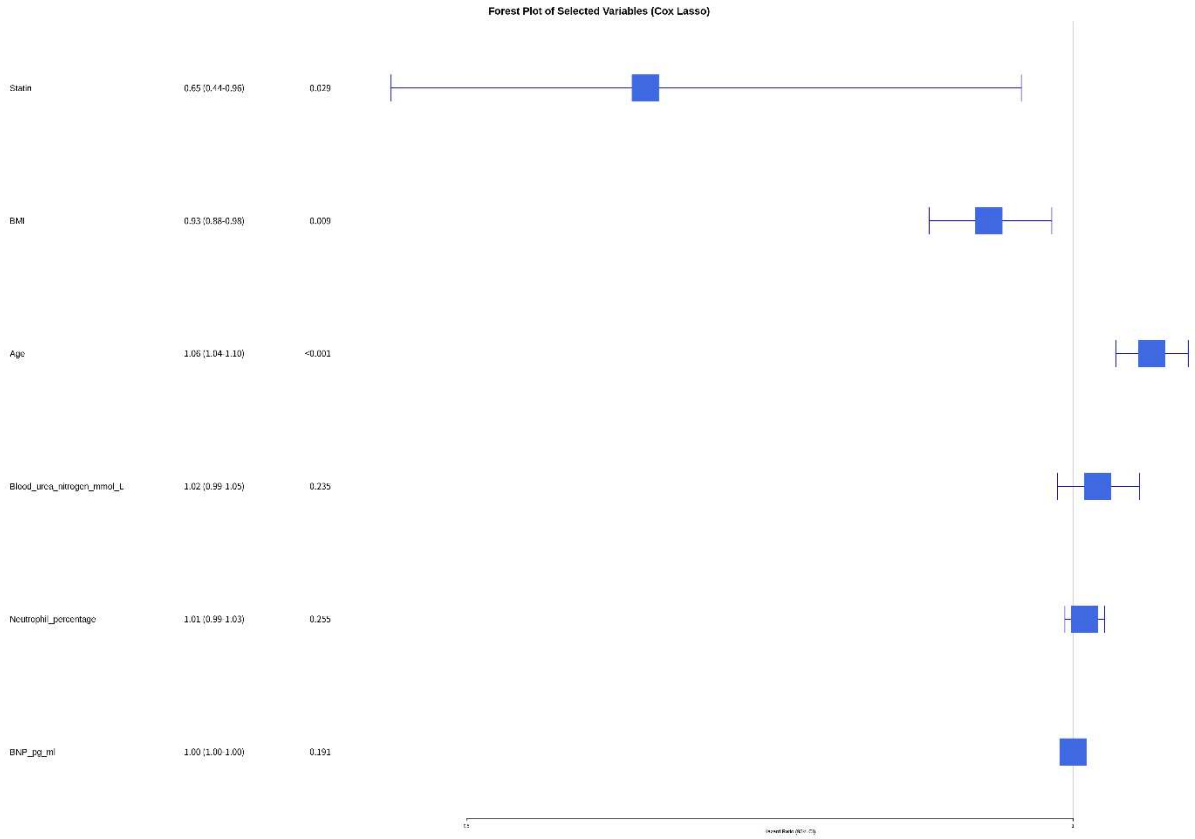


Figure 3. Forest plot of selected variables in the BMI LASSO-Cox model.

Hazard ratios (squares) and 95% confidence intervals (horizontal lines) are shown. A hazard ratio <1 indicates a protective effect. BMI and statin use are significantly protective, while age is a significant risk factor.

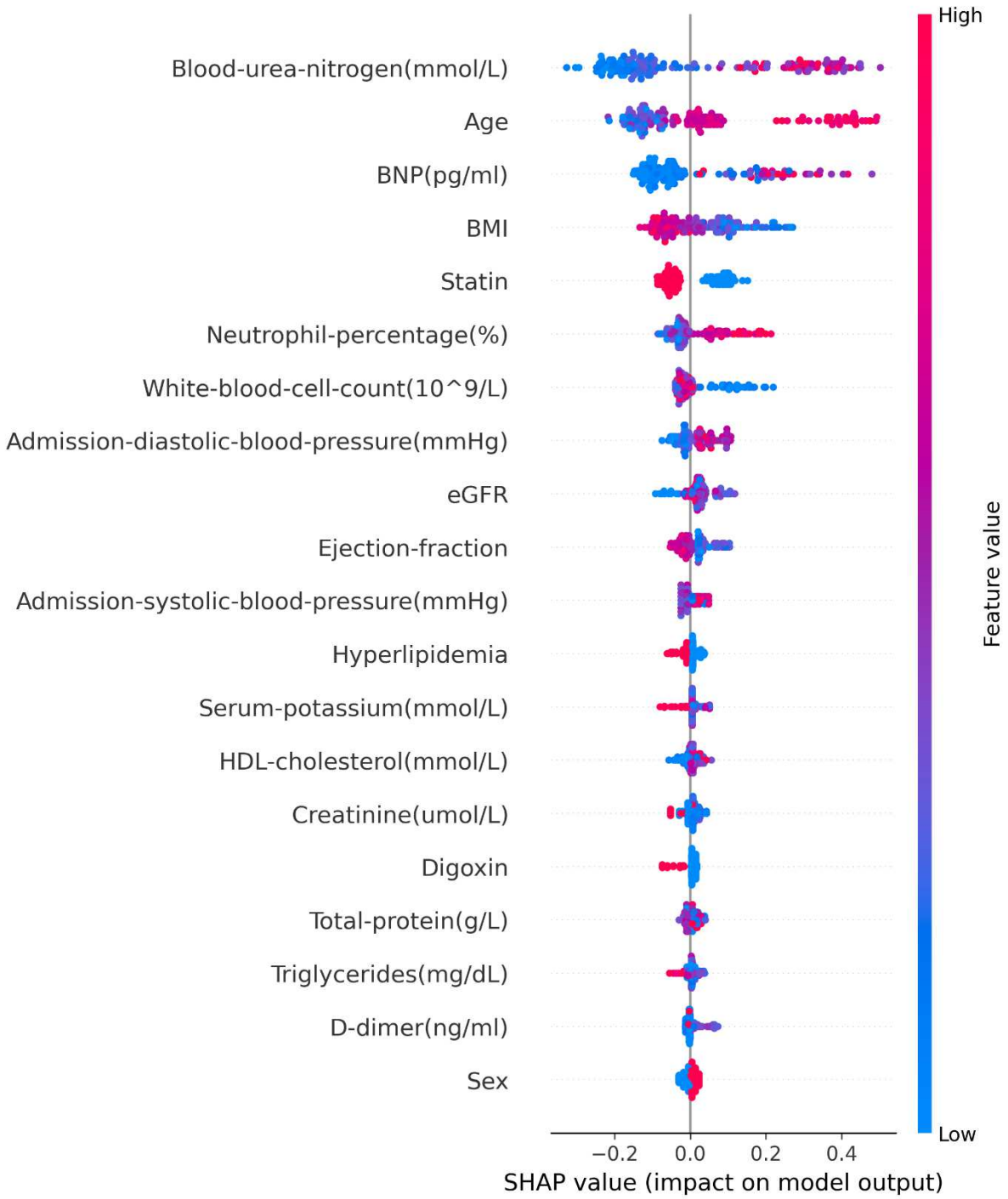


Figure 4. SHAP summary plot for the BMI-based XGBoost model

Variables are ranked by mean absolute SHAP values. Higher SHAP values indicate greater influence on model predictions. BUN, age and BNP are the top contributors; BMI ranks fifth with a mean SHAP of 0.08.

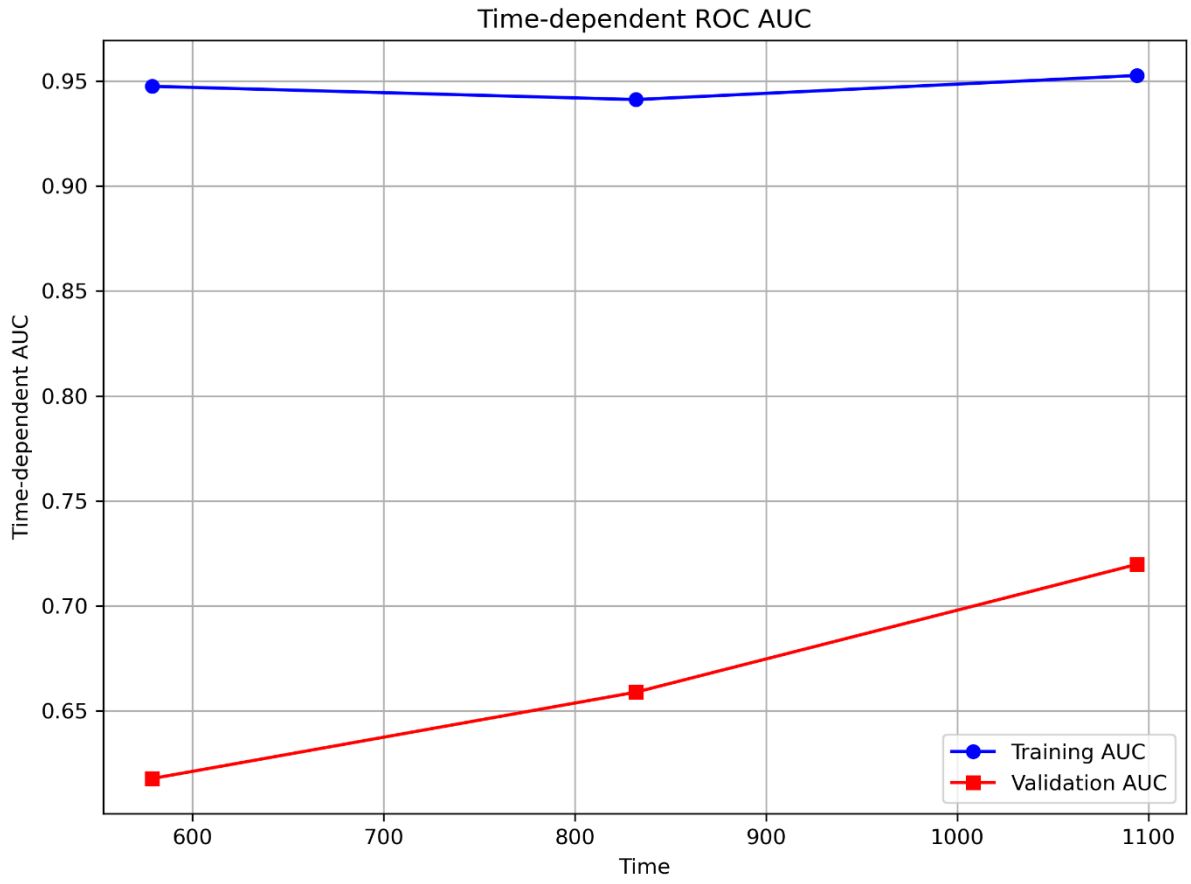


Figure 5. Time-dependent AUC curves for the BMI-based XGBoost model

Training AUC (blue) remains consistently high (0.95–0.96) across follow-up, while validation AUC (red) increases from 0.62 to 0.72, with a mean validation AUC of 0.65.

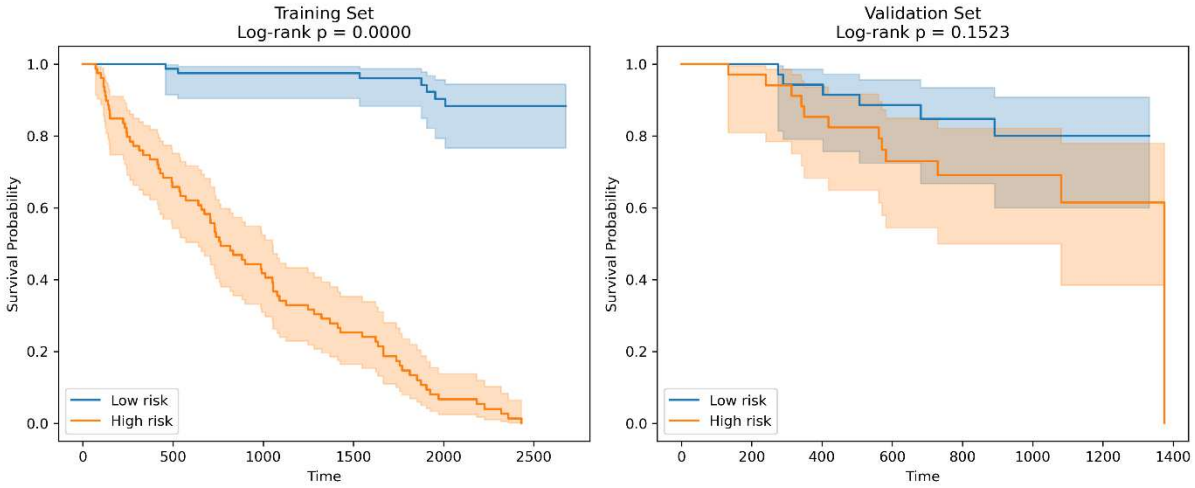


Figure 6. Kaplan-Meier risk stratification for the BMI-based XGBoost model.

Patients are dichotomised into high- and low-risk groups using the median XGBoost risk score. The training cohort shows a highly significant separation (log-rank $p < 0.001$), whereas the validation cohort exhibits a non-significant trend ($p = 0.15$).

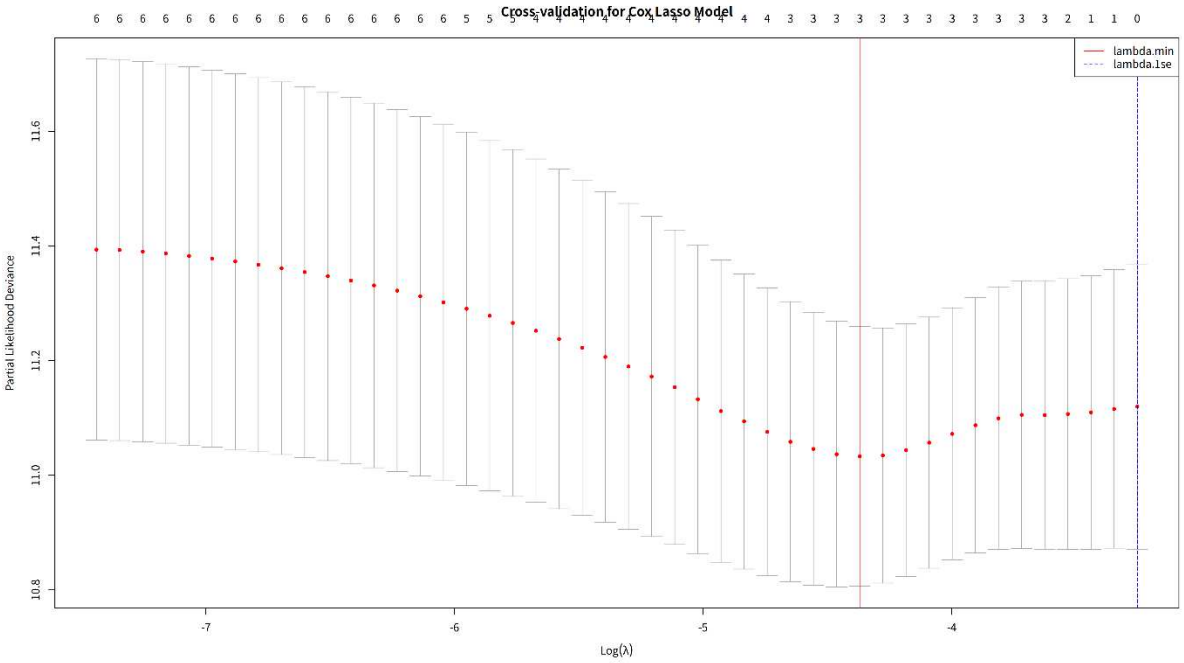


Figure 7. Cross-validation curve for lambda selection in Lasso-penalized Cox regression.

The x-axis shows the log(λ) values, while the y-axis represents the partial likelihood deviance with standard error bars from 10-fold cross-validation. The red vertical line indicates λmin (0.0127), and the blue dashed line indicates λ1se (0.0386). At λmin, the model retains 3 non-zero coefficients, optimizing the bias-variance tradeoff.

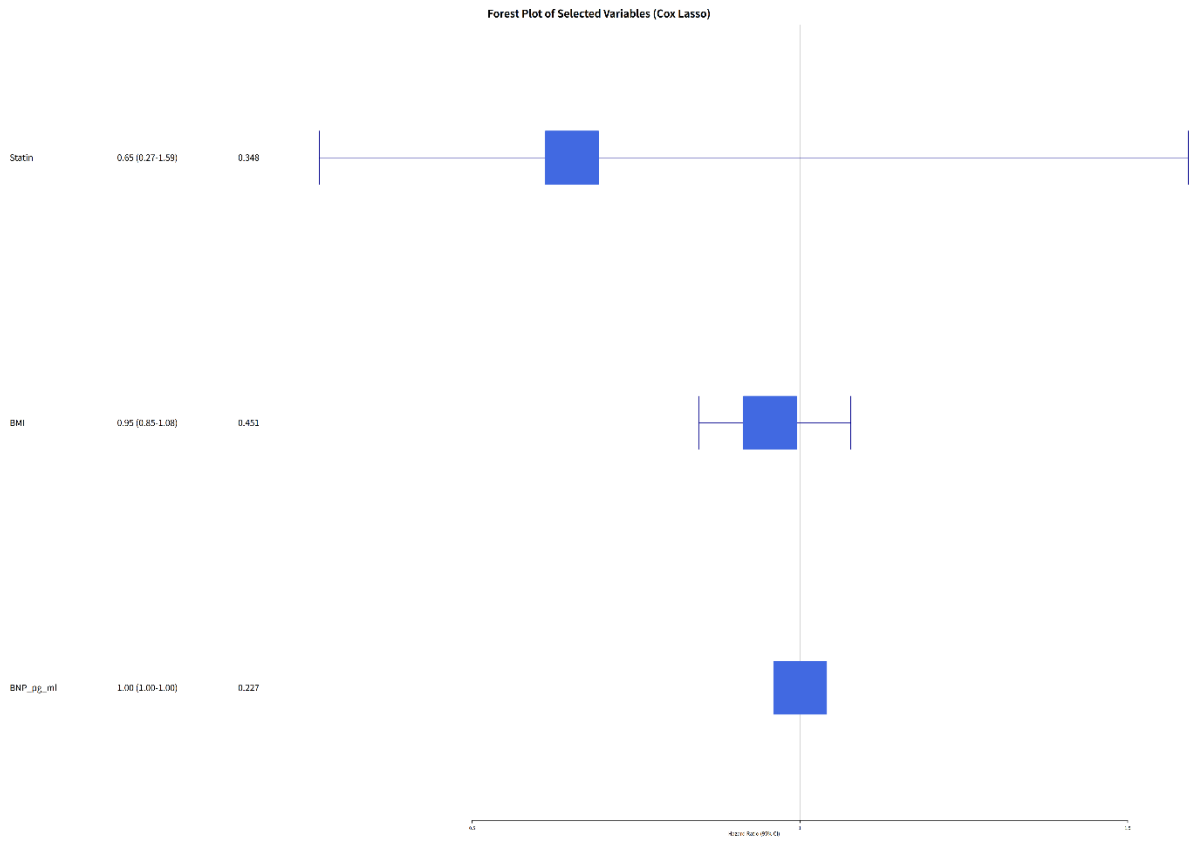


Figure 8. Forest plot of hazard ratios for selected predictors in the multivariate Lasso-Cox model.

The plot displays hazard ratios (squares) with 95% confidence intervals (horizontal lines). The vertical dashed line represents HR = 1 (no effect). None of the predictors reached statistical significance ($P > 0.05$).

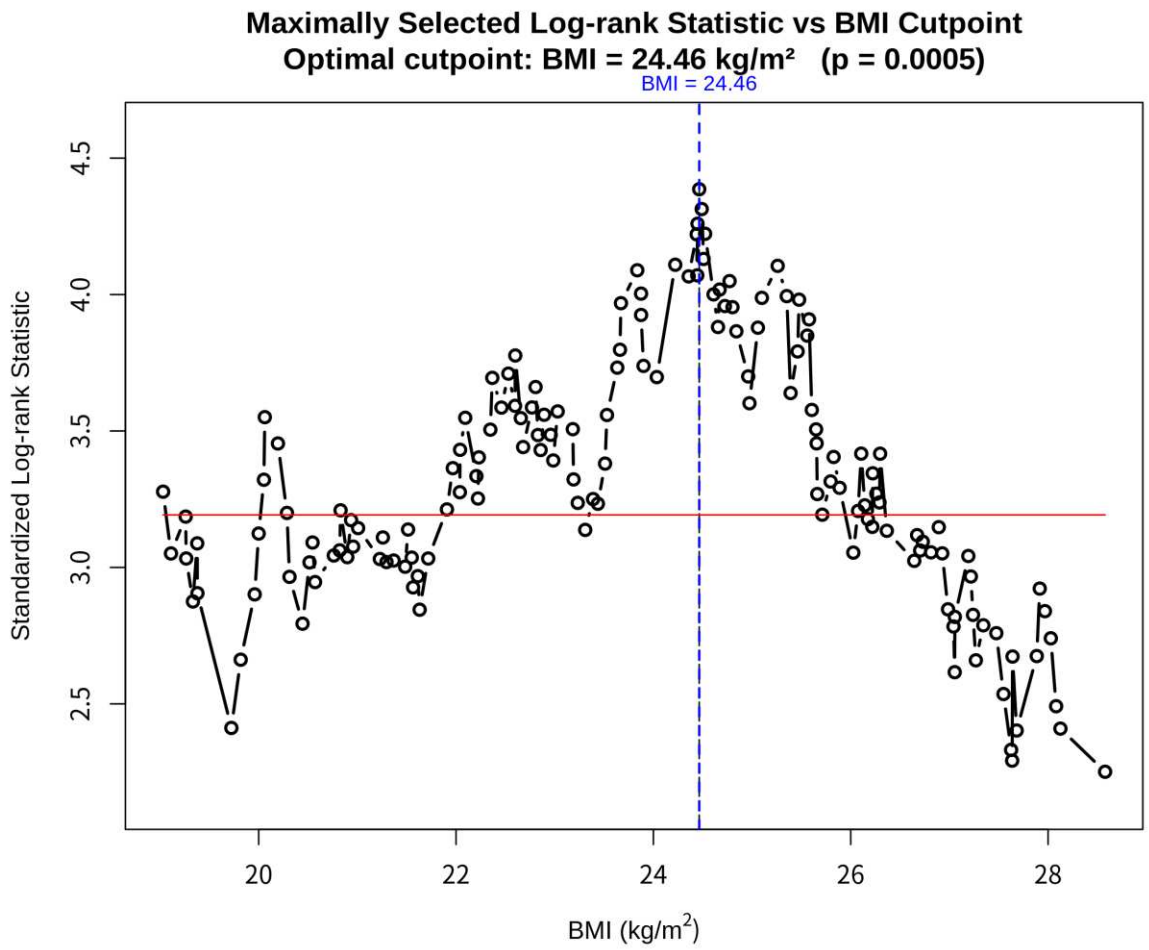


Figure 9. Maximally selected log-rank statistic for BMI cut-point identification.

The x-axis represents candidate BMI cut-points (kg/m²), and the y-axis shows the standardized log-rank statistic. The blue dashed line marks the optimal cut-point at 24.46 kg/m², which yields the maximum statistic (peak). The red horizontal line indicates the significance boundary at $\alpha = 0.05$ after Lau94 correction for multiple testing. The peak exceeding the red line confirms that the identified cut-point provides a statistically significant separation of survival outcomes (corrected $P = 0.00053$).

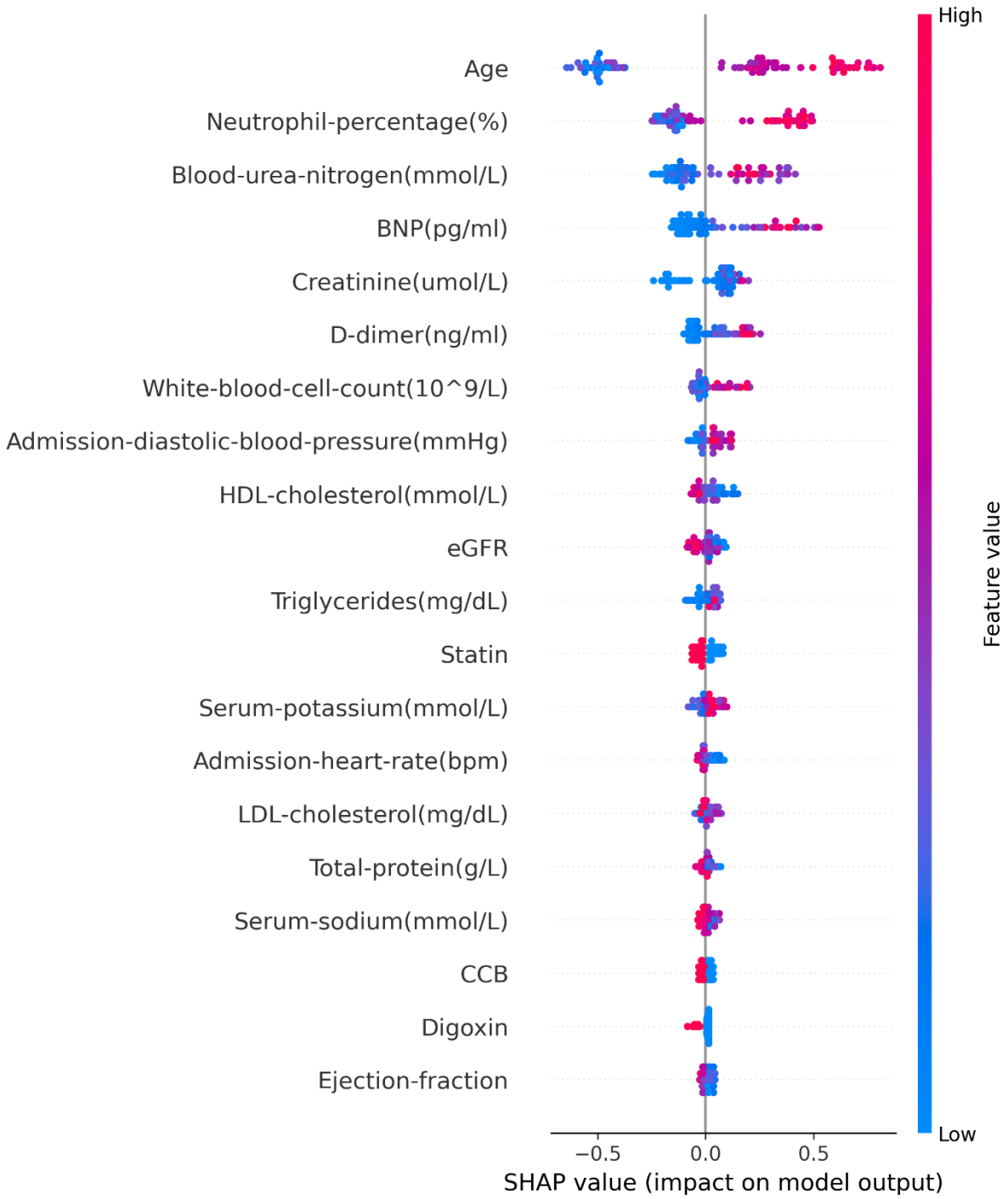


Figure 10. SHAP Feature Importance Analysis Comparing Both BMI Groups.

SHAP (SHapley Additive exPlanations) summary plots showing the mean absolute SHAP values for each clinical predictor. Low BMI group (BMI < 24.46 kg/m²): BUN ranks as the 3rd most important feature (SHAP = 0.18), highlighting its strong prognostic value in this subgroup.

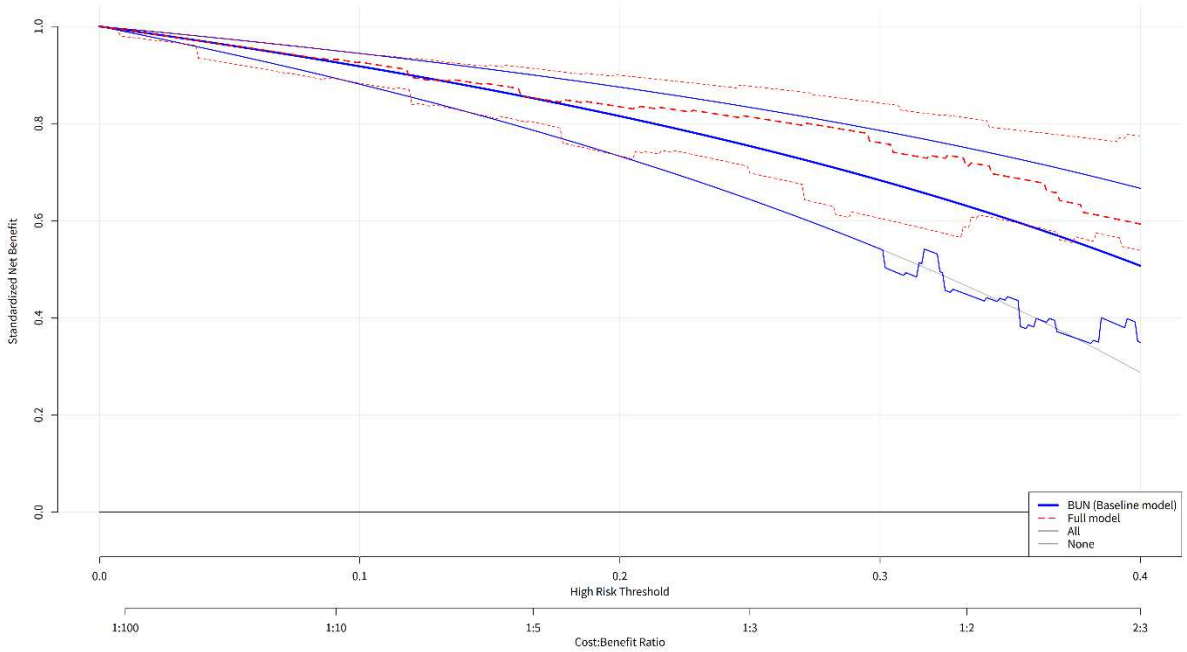


Figure 11. Decision curve analysis comparing BUN-only baseline model versus full model (BUN + Age + Neutrophil percentage + BNP + Creatinine) for predicting all-cause mortality in elderly HFpEF patients with low BMI.

The y-axis shows standardized net benefit, and the x-axis represents the threshold probability.

TABLE

Table 1. Baseline characteristics of elderly HFpEF patients (≥65 years) stratified by all-cause mortality during a median follow-up of 2–3 years

Variable	Survivors (n=125)	Non-survivors (n=103)	P-value
Demographics			
Age (years)	80.26 ± 8.06	85.60 ± 7.50	<0.001 ***
Sex, male (%)	78 (62.40)	75 (72.82)	0.127 ns
Body weight (kg)	68.10 ± 11.78	62.88 ± 12.17	0.001 **
BMI (kg/m²)	24.88 ± 3.46	22.80 ± 3.84	<0.001 ***
Vital signs			
Admission SBP (mmHg)	140.49 ± 22.36	139.53 ± 23.58	0.756 ns
Admission DBP (mmHg)	74.06 ± 12.73	72.62 ± 13.12	0.403 ns
Admission heart rate (bpm)	78.09 ± 17.79	77.18 ± 16.40	0.691 ns
Cardiac function			

Variable	Survivors (n=125)	Non-survivors (n=103)	P-value
Ejection fraction (%)	56.94 ± 4.34	55.65 ± 2.84	0.007 **
BNP (pg/ml)	367.91 ± 585.02	607.20 ± 765.80	0.010 *
Comorbidities			
Hypertension (%)	100 (80.00)	86 (83.50)	0.613 ns
Atrial fibrillation (%)	46 (36.80)	28 (27.18)	0.161 ns
Diabetes mellitus (%)	39 (31.20)	34 (33.01)	0.882 ns
Chronic kidney disease (%)	26 (20.80)	40 (38.83)	0.004 **
COPD (%)	16 (12.80)	15 (14.56)	0.847 ns
Stroke (%)	14 (11.20)	14 (13.59)	0.730 ns
Hyperuricemia (%)	12 (9.60)	15 (14.56)	0.343 ns
Hyperlipidemia (%)	45 (36.00)	30 (29.13)	0.338 ns
Medications			

Variable	Survivors (n=125)	Non-survivors (n=103)	P-value
ACEI (%)	9 (7.20)	4 (3.88)	0.431 ns
ARB (%)	41 (32.80)	24 (23.30)	0.152 ns
Beta-blocker (%)	74 (59.20)	49 (47.57)	0.105 ns
CCB (%)	56 (44.80)	46 (44.66)	1.000 ns
Digoxin (%)	14 (11.20)	8 (7.77)	0.517 ns
Statin (%)	94 (75.20)	47 (45.63)	<0.001 ***
MRA (%)	54 (43.20)	45 (43.69)	1.000 ns
Antiplatelet agent (%)	78 (62.40)	47 (45.63)	0.016 *
Anticoagulant (%)	23 (18.40)	8 (7.77)	0.033 *
Laboratory data			
White blood cell count ($\times 10^9$/L)	6.88 ± 2.87	6.80 ± 2.46	0.818 ns
Neutrophil percentage (%)	65.52 ± 12.33	70.29 ± 14.32	0.008 **

Variable	Survivors (n=125)	Non-survivors (n=103)	P-value
D-dimer (ng/ml)	468.24 ± 891.25	620.72 ± 875.12	0.196 ns
Serum sodium (mmol/L)	138.96 ± 3.94	138.11 ± 4.22	0.118 ns
Serum potassium (mmol/L)	4.04 ± 0.47	4.25 ± 0.63	0.005 **
Creatinine (μmol/L)	129.30 ± 157.20	183.18 ± 179.33	0.018 *
Blood urea nitrogen (mmol/L)	8.62 ± 5.05	11.69 ± 8.14	0.001 **
eGFR (ml/min/1.73m²)	86.63 ± 53.12	63.11 ± 42.15	<0.001 ***
Total protein (g/L)	65.60 ± 5.67	65.56 ± 6.89	0.962 ns
Prealbumin (mg/L)	209.04 ± 62.91	196.25 ± 66.22	0.139 ns
Triglycerides (mmol/L)	1.36 ± 0.76	1.30 ± 0.79	0.554 ns
Total cholesterol (mmol/L)	3.80 ± 0.98	4.08 ± 1.04	0.039 *
LDL-cholesterol (mg/dL)	2.16 ± 0.75	2.32 ± 0.75	0.109 ns
HDL-cholesterol (mmol/L)	1.09 ± 0.29	1.13 ± 0.38	0.401 ns

Variable	Survivors (n=125)	Non-survivors (n=103)	P-value
Hemoglobin (g/L)	119.48 ± 20.26	109.83 ± 22.79	<0.001 ***
Platelet count (×10⁹/L)	179.78 ± 62.16	177.47 ± 68.73	0.792 ns
Albumin (g/L)	39.88 ± 4.15	38.87 ± 4.44	0.081 ns
Lymphocyte count (×10⁹/L)	1.46 ± 0.69	1.43 ± 2.64	0.924 ns
Nutritional scores			
HALP score	44.15 ± 28.64	39.28 ± 72.12	0.520 ns
TCBI	122.94 ± 99.00	110.52 ± 76.91	0.288 ns
GNRI	100.22 ± 6.77	97.15 ± 8.03	0.002 **
CONUT score	4.37 ± 1.58	4.88 ± 1.33	0.009 **
PNI	47.17 ± 5.62	46.03 ± 14.12	0.444 ns
Albumin score	0.27 ± 0.93	0.39 ± 0.89	0.347 ns
Lymphocyte count score	1.17 ± 1.09	1.58 ± 1.03	0.004 **

Notes: Data are presented as mean ± SD for continuous variables and n (%) for categorical variables. P-values were derived from independent t-test (continuous) or chi-square test (categorical). Significance: *** p<0.001; ** p<0.01; * p<0.05; ns, not significant.*

Abbreviations: HFpEF, heart failure with preserved ejection fraction; BMI, body mass index; SBP, systolic blood pressure; DBP, diastolic blood pressure; BNP, B-type natriuretic peptide; COPD, chronic obstructive pulmonary disease; ACEI, angiotensin-converting enzyme inhibitor; ARB, angiotensin receptor blocker; CCB, calcium channel blocker; MRA, mineralocorticoid receptor antagonist; eGFR, estimated glomerular filtration rate; LDL, low-density lipoprotein; HDL, high-density lipoprotein; HALP, hemoglobin-albumin-lymphocyte-platelet; TCBI, total cholesterol–body weight index; GNRI, geriatric nutritional risk index; CONUT, controlling nutritional status; PNI, prognostic nutritional index.

Table 2. Comparison of LASSO-Cox model results for BMI and other nutritional indices in predicting all-cause mortality among elderly HFpEF patients

Nutritional index	HR (95% CI) for index	P value	HR (95% CI) for age (per year)	P value	HR (95% CI) for statin use	P value
BMI	0.93 (0.88–0.98)	0.009	1.06 (1.04–1.09)	<0.001	0.65 (0.44–0.96)	0.029
HALP	Not selected	1	1.06 (1.03–1.09)	<0.001	0.69 (0.46–1.03)	0.068
TCBI	Not selected	1	1.07 (1.04–1.10)	<0.001	0.61 (0.41–0.89)	0.01
GNRI	0.98 (0.95–1.02)	0.31	1.07 (1.04–1.10)	<0.001	0.62 (0.42–0.91)	0.016
CONUT	Not selected	1	1.05 (1.03–1.08)	<0.001	0.70 (0.49–1.02)	0.06
PNI	1.00 (0.97–1.03)	1	1.07 (1.04–1.10)	<0.001	0.62 (0.43–0.91)	0.015

Notes: “Not selected” indicates the LASSO penalty shrunk the coefficient to zero at λ.min; thus no HR or CI is estimated. Age and statin HRs are derived from the respective model for each nutritional index.

Table 3. Model performance and BUN feature importance in XGBoost-based risk stratification stratified by BMI subgroups among elderly HFpEF patients.

Parameter	Low BMI Group (<24.46)	High BMI Group (≥24.46)

Sample Size		120		108
Training Samples / Events	84 / 56		75 / 29	
Validation Samples / Events	36 / 13		33 / 5	
Training C-index		0.94		0.91
Validation C-index		0.68		0.44
BUN SHAP Rank / Value	3rd / 0.18		10th / 0.05	